Lignes d’ancrage en fibre synthétiques

De l’approche théorique à l’application pour des éoliennes offshore flottantes

Laure Civier

Ingénieure de recherche en ancrage innovants

Table of contents

France Energies Marines en bref

Institut de recherche et d'innovation
sur l'éolien en mer
reconnu pour son impact industriel, économique et sociétal

FRANCE ENERGIES MARINES

100 collaborateurs

Depuis **2012**

10 M€ d'activité en 2024

Siège à **Brest**
Antennes au **Havre**, **Nantes** et **Marseille**

ITE soutenu par les
le plan d'investissement
France 2030

Un partenariat public-privé

Actionnariat
50 % public
50 % privé

SAS avec
un capital de
699 000 €

La R&D pour transformer les enjeux de viabilité en innovations

FRANCE ENERGIES MARINES

Les enjeux de la filière

- Changement d'**échelle**
- Renforcement de la chaîne **logistique** et des **compétences**
- Objectivisation des **impacts**
- **Fiabilisation** et **dimensionnement** des systèmes
- Maîtrise des **coûts** d'O&M
- **Viabilité** économique de l'éolien flottant

Notre mission

- **Consolider** les standards et logiciels de référence pour qualifier la ressource et les conditions d'opération des parcs
- **Développer** des outils opérationnels pour fiabiliser, dimensionner et maîtriser l'OPEX
- **Elaborer** des outils de référence pour optimiser l'intégration environnementale et socio-économique des parcs

Notre feuille de route scientifique et technologique

FRANCE ENERGIES MARINES

CARACTÉRISATION DE SITES

- Spatialisation des observations
- Caractérisation des états de mer
- Caractérisation du vent en mer
- Changement climatique
- Processus hydrosédimentaires

DIMENSIONNEMENT ET SUIVI DES SYSTÈMES

- Structure, ancrages et câble électrique
- Couplage hydrodynamique et structure
- Jumeaux numériques et suivi en service
- Innovation technologique

4 programmes de R&D
transversaux et complémentaires

INTÉGRATION ENVIRONNEMENTALE

- Effets sur les compartiments de l'écosystème
- Changement d'échelle socio-écosystémique, spatiale et temporelle
- Outils pour l'intégration environnementale

OPTIMISATION DES PARCS

- Architecture de ferme
- Intégration aux réseaux (hydrogène…)
- Installation, opération et maintenance

Un comité scientifique & technologique indépendant

FRANCE ENERGIES MARINES

UNIVERSITY OF PLYMOUTH

Deborah GREAVES

NTNU

Erin BACHYNSKI-POLIĆ

NREL
NATIONAL RENEWABLE ENERGY LABORATORY

Emmanuel BRANLARD

THE UNIVERSITY of EDINBURGH

Claire HAGGETT

Caractérisation de sites

Dimensionnement et suivi des systèmes
Optimisation des parcs

Intégration environnementale

Xiaoli GUO LARSÉN

DTU

Hannele HOLTTINEN

recognis

Thomas Michel SAUDER

SINTEF

Lenaïg HEMERY

Pacific Northwest
NATIONAL LABORATORY

Table of contents

Industrial context

FRANCE ENERGIES MARINES

Need to find innovative mooring systems for floating offshore wind turbines

Oil platform P-51 off the Brazilian coast is a semi-submersible platform.
Divulgação Petrobras / ABr - Agência Brasil [1]

The Floatgen floating wind turbine, equipped with the Ideol float, installed on the SEM-REV (Centrale Nantes) off Le Croisic.
Credits: Ideol / V. Joncheray

FRANCE ENERGIES MARINES

Need to find innovative mooring systems for floating offshore wind turbines

Systèmes d'ancrage:

Fonction principale: maintien du flotteur à une position donnée avec une certaine tolérance et avec une certaine souplesse

Fonction secondaire: contribuer à l'amortissement des mouvements

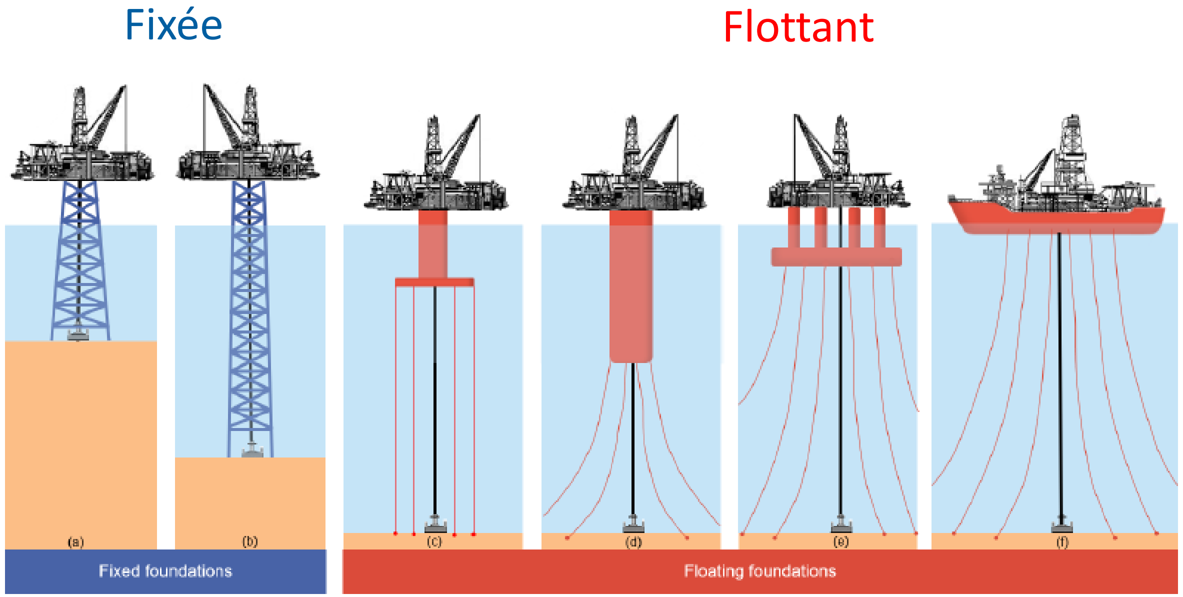

Type d'ancrage: défini par le nombre de lignes, la disposition des lignes d'ancrage et par la composition de celles-ci.

Giovani Aiosa do Amaral. Analytical assessment of the mooring system stiffness. March 2020.

Industrial context

FRANCE ENERGIES MARINES

Need to find innovative mooring systems for floating offshore wind turbines

Figure 5 – Offshore Oil & Gas Platforms: (a) fixed, (b) compliant, (c) Tension-leg, (d) Spar, (e) Semi-submersible and (f) Floating Production Storage and Offloading (FPSO).

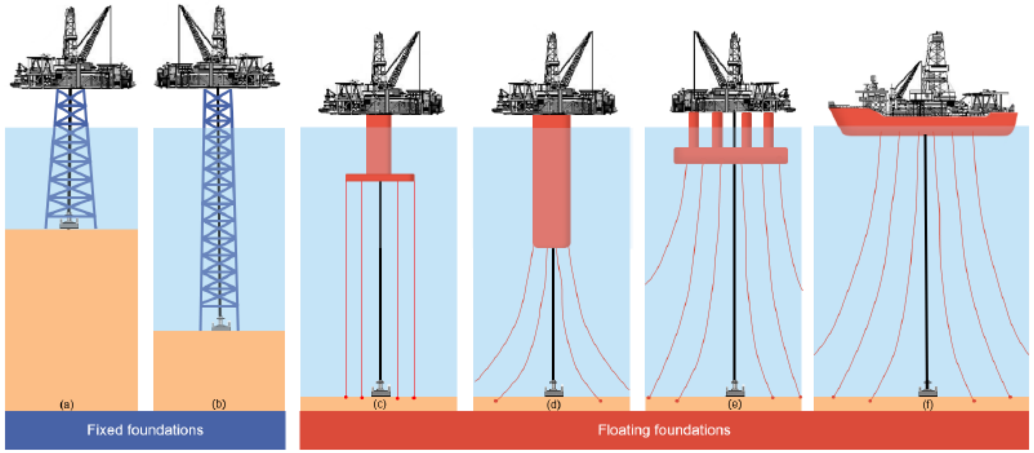

Giovani Aiosa do Amaral. Analytical assessment of the mooring system stiffness. March 2020.

0 à 60m | Au-delà de 60 mètres

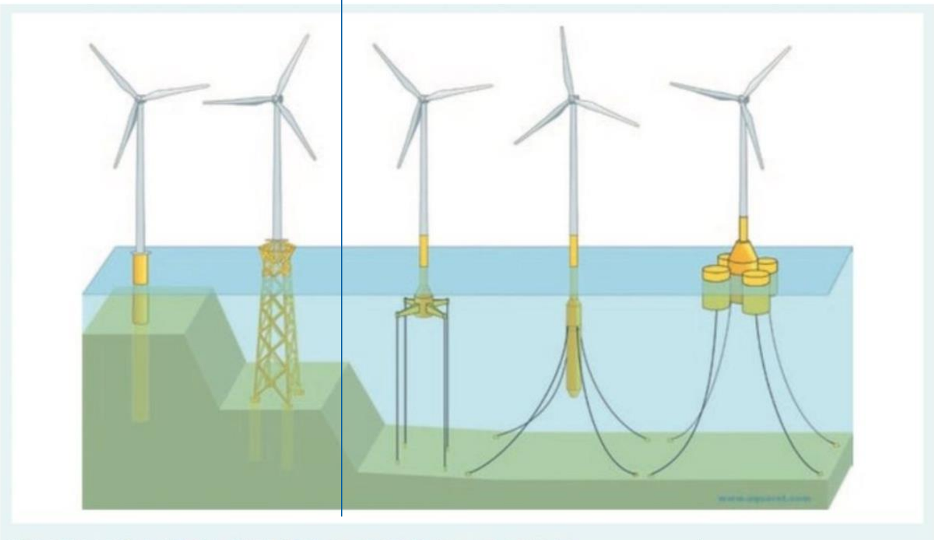

Figure 1: Common fixed and floating offshore wind structure designs (Source: www.aquaret.com). From left to right: driven monopile; steel jacket tower; tension leg platform; spar buoy; semi-submersible

Hannon, M et al (2019) Offshore wind, ready to float? Global and UK trends in the floating offshore wind market. University of Strathclyde, Glasgow, https://doi.org/10.17868/69501

Mooring of a floating platform

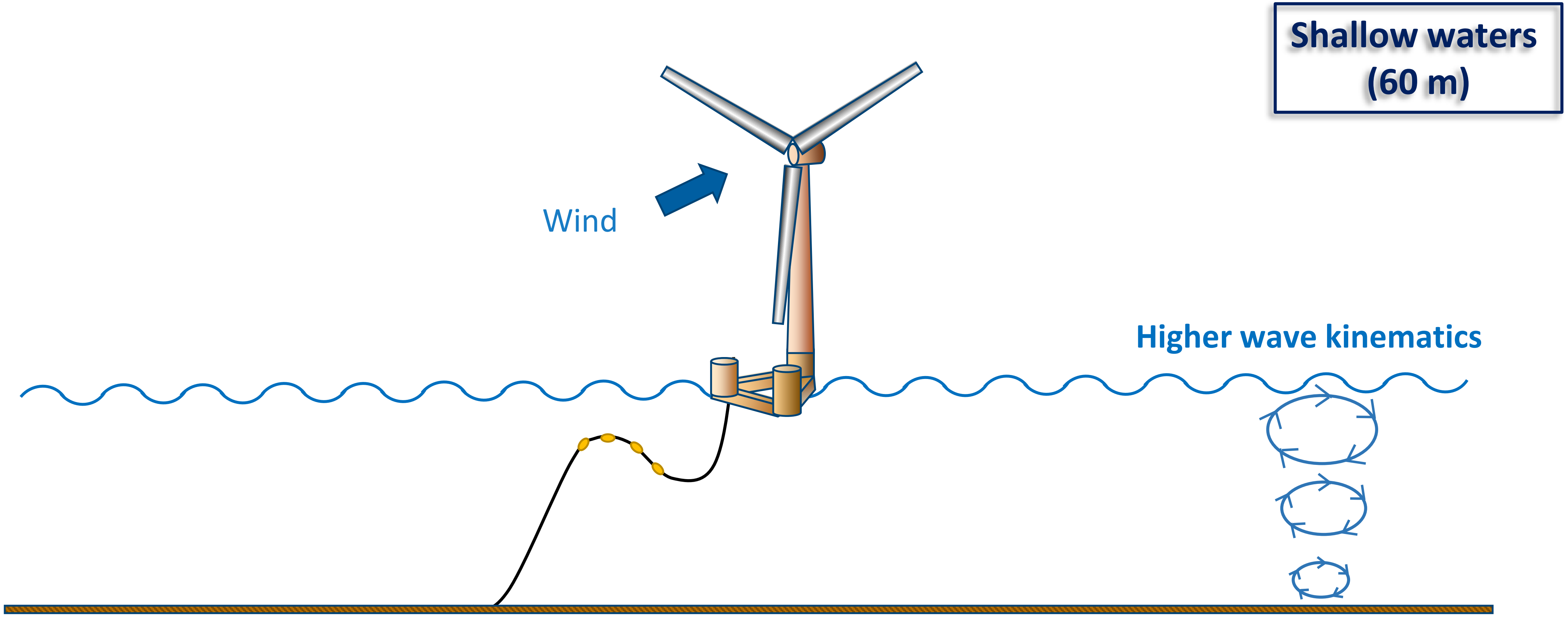

Mooring of a floating platform

FRANCE ENERGIES MARINES

- The export cable integrity should be maintained with limited floater offsets

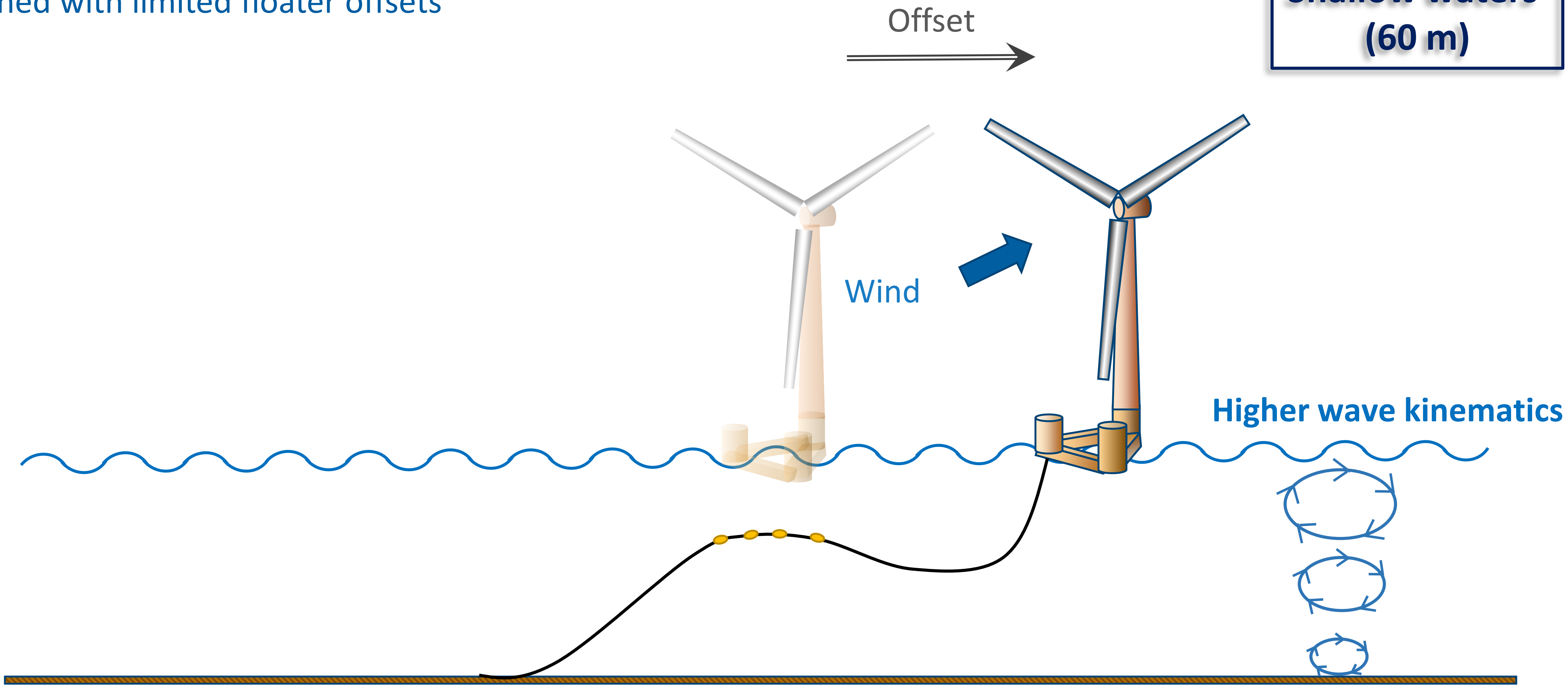

Mooring of a floating platform

- ✓ The export cable integrity should be maintained with limited floater offsets
- ✓ Structural loadings are damped using low stiffness mooring systems

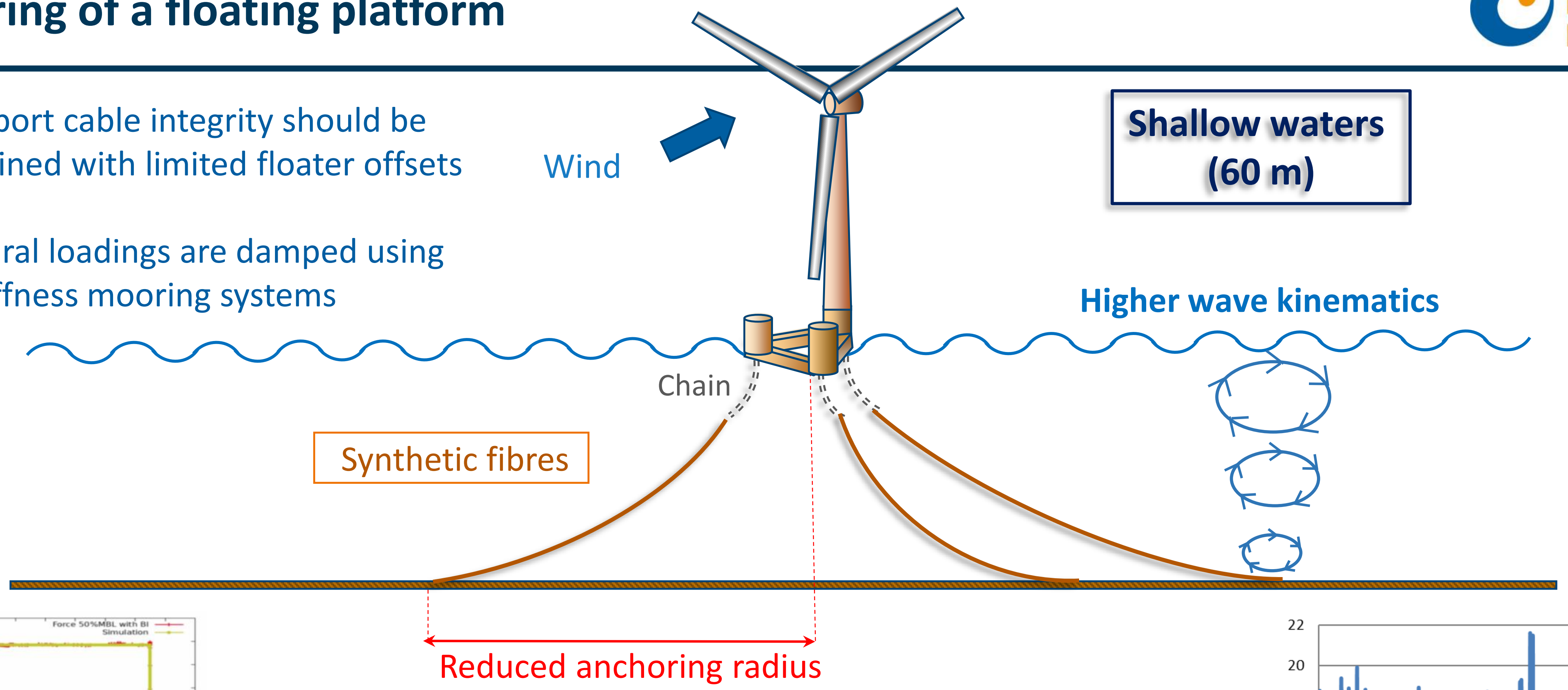

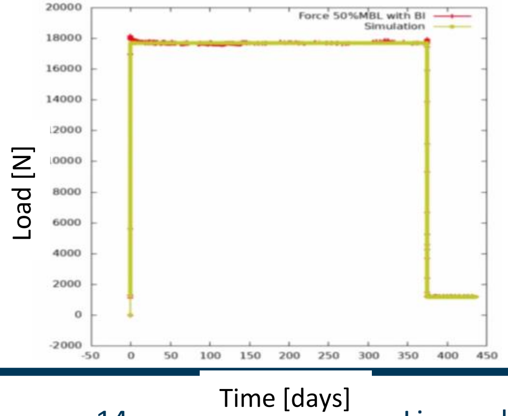

Long term creep loading

Stochastic loading

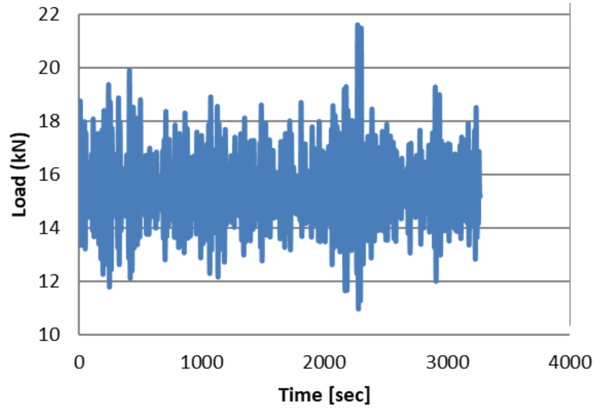

Mooring lines: synthetic fibres ropes

- Polyester, aramid, HMPE, nylon
- Non linear axial stiffness characteristic
- Reduction weight
- High resistance
- Possible reduction in installation cost
- Lack of long term service experience
- Used in permanent or temporary deep-water moorings and for mooring of wind turbines

Typical stress-strain behavior of available synthetic fibres:

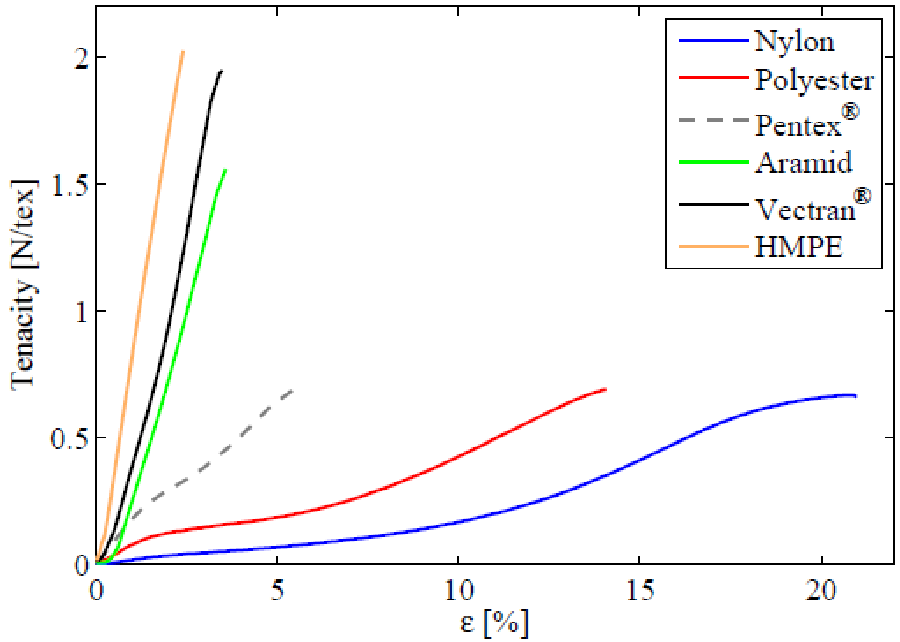

Weller, S., Davies, P., Vickers, A., Johanning, L., 2014. Synthetic rope responses in the context of 593 load history: Operational performance. Ocean Engineering 83, 111–124. URL: 594

Mooring line: flexible synthetic fibre ropes

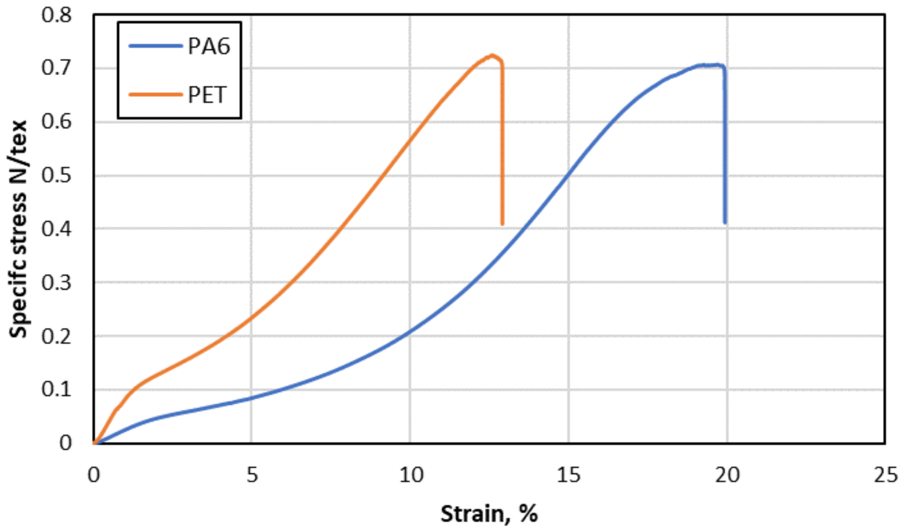

		Nylon 6	Polyester
Durability	Ultraviolet light	Good	Good
	Chemicals	Good	Good
	Temperature	Good	Good
	Abrasion	Average	Good
	Creep	Average	Good
	Tension fatigue	Good	Good
	Compression fatigue	Good	Good

Weller, S *et al*. 2015.

Polyester (PET)

Advantages:

- High tension strength
- Fatigue resistance
- Known behaviour

But : Too stiff for shallow waters

Polyamide 6 (Nylon)

Advantages:

- Less stiff
- Good tension strength
- High strain to failure (20%)
- Affordable

But: Only used for short term applications: 2 years.

Research challenges included in the research projects:

- Long term creep behavior
- Development of a 3D multi-scale model
- Fatigue life and durability
- 1D constitutive law

Mooring project lead by FEM

2017

Projet POLYAMOOR

Thèse Y. Chevillotte

2020

Projet MONAMOOR

Thèse L. Civier et Post Doc C. Bain

2023

2027

Projet BAMOS Thèse

Institut de Recherche Dupuy de Lôme UMR CNRS 6027

Multi-scale material

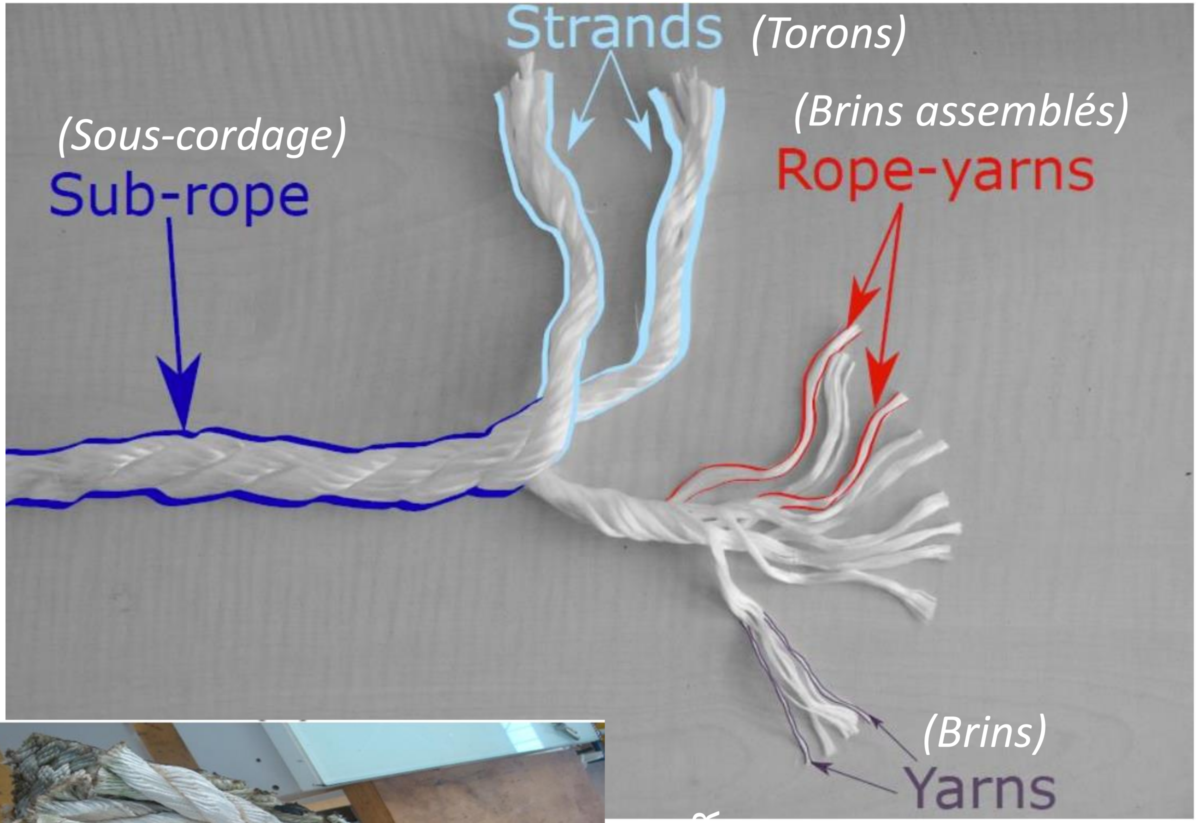

BEXCO

Fig: Composition of a polyamide 6 4T sub-rope supplied by BEXCO, Belgium

Important parameters of the construction:

- Lay-angle/Lay-length
- Number of components in each scale
- Diameter
- Coating

Scale:

Laboratory scale: 4T (lay-length: 50 mm)
Full scale: around 30T

Specificities:

- Size of a rope usually defined by its linear density

Textile units : $tex = g/km$

- All ropes have voids
  - Difficult to measure a section
  - Nominal specific stress (N/tex)
  - $1\ N/tex \approx 1\ GPa$ (average rope)
- Usually mechanical value given in % of Minimal Breaking Load (MBL)

Table of contents

Context and state of the art

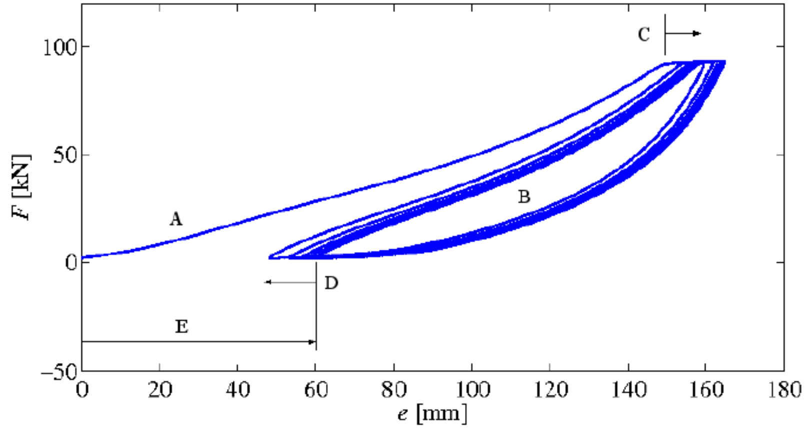

- The non-linearity and complex behavior of polyamide 6 (visco-elasto-plastic behavior)
- The need to describe and predict this complex behavior for mooring lines application

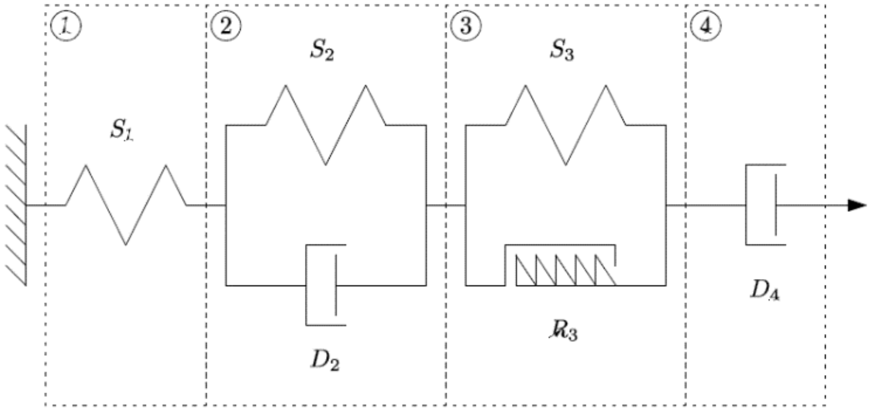

- Flory's model that helped developed the POLYAMOOR law
- François and Davies model (2008) with mean elongation, quasi-static stiffness
- Dynamic response

Context and state of the art

- Model of the elongation-tension relation of mooring line:
  - Usually developed at the scale of the sub-rope
  - Classic method: static stiffness and dynamic stiffness (dedicated tensile tests of BV, DNV …)
- Issue: some mechanical phenomena are ignored:
  - Permanent elongation (dependent on max. tension)
  - Viscosity (long-term creep, stochastic loading)
  - Loading history dependence (impact of a storm)
- Possible solution = visco-elasto-plastic behavior law of the sub-rope in tension:
  - Syrope spring-dashpot law (polyester sub-rope, no direct identification method)
  - 1D POLYAMOOR visco-elasto-plastic law (polyamide sub-rope, efficient identification method)

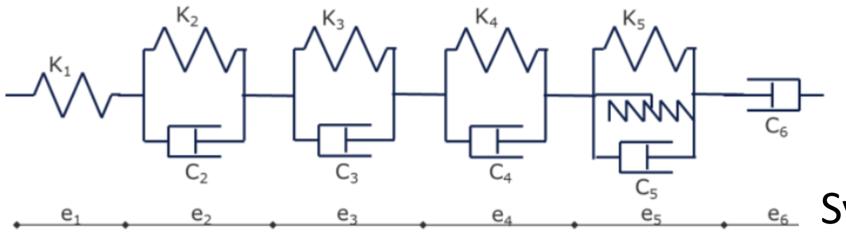

FIGURE 8: Adjusted spring-dashpot model

Syrope law
(Falkenberg et al., 2017)

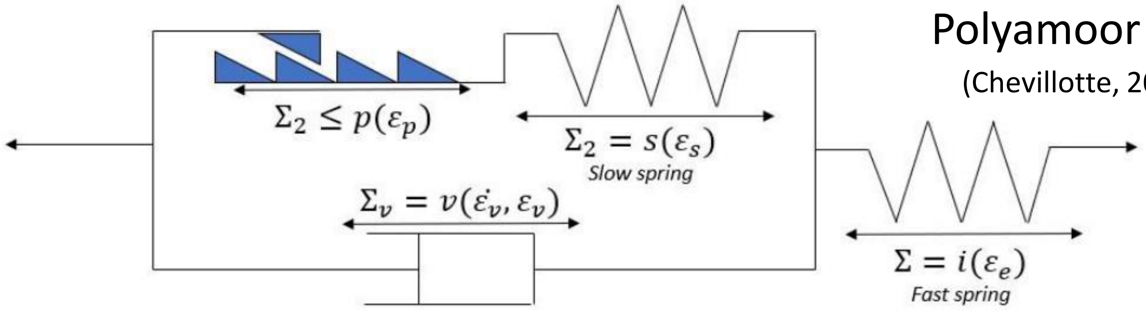

Figure 3.2 - The POLYAMOOR constitutive law

Polyamoor law
(Chevillotte, 2020)

POLYAMOOR law description

→ **Constitutive law developed on 4T scale polyamide sub-rope for floating offshore wind turbines moorings**

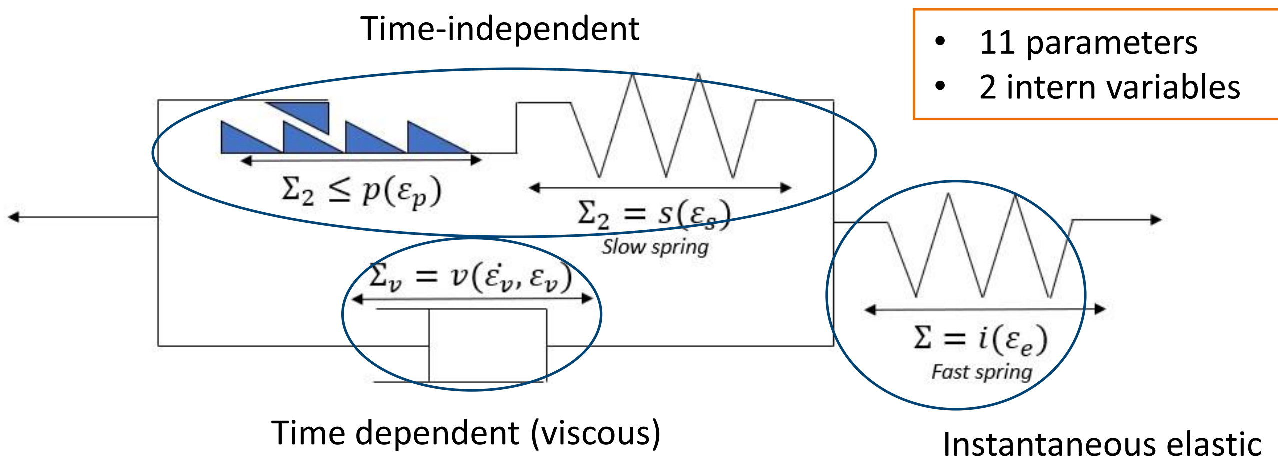

- 11 parameters
- 2 intern variables

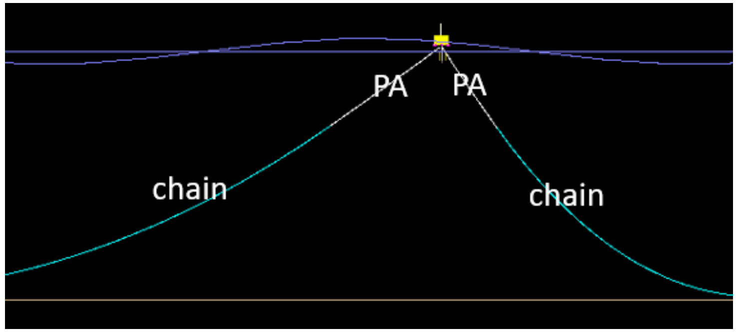

Logiciel DeepLines basé la méthode d'éléments finis dans lequel une première version de la loi POLYAMOOR est implémentée

With the POLYAMOOR law, we aim at:

- Describing the behavior of nylon 6 and taking into account: the history of loading, fatigue anc cyclic response, creep, relaxations.

POLYAMOOR law description

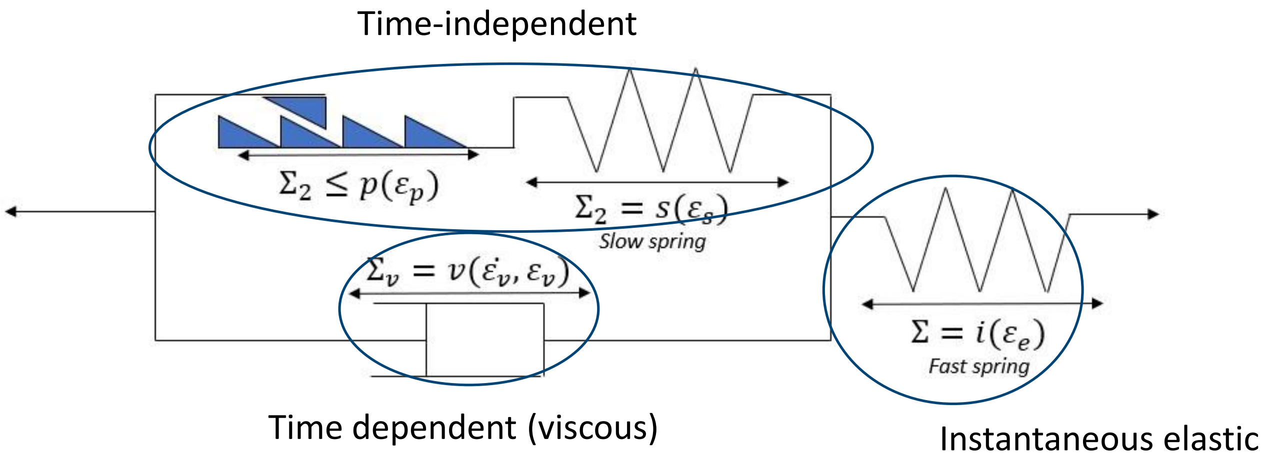

- 11 parameters
- 2 intern variables

The one-dimensional spring-dashpot-ratchet law is represented in and has the following elements:

- **A fast spring** describing the dynamic behavior,
- **A dashpot** responsible for the viscous stress of the polymer,
- A time-independent part consisting of a **ratchet element** for the plasticity, and a **slow spring** responsible for the relaxed elasticity.

$$i(\varepsilon) = \frac{b}{a} \cdot (e^{a \cdot \varepsilon} - 1)$$

a [-]
b [N/tex]

$$d(\varepsilon) = \frac{g}{c} \cdot (e^{c \cdot \varepsilon} - 1)$$

c [-]
g [N/tex]

$$p(\varepsilon_p) = e \cdot (\tanh(f \cdot \varepsilon_p + h) + 1) \text{ if } \varepsilon_p \leq \frac{-h}{f}$$
$$p(\varepsilon_p) = e \cdot (f \cdot \varepsilon_p + h + 1) \text{ if } \varepsilon_p > \frac{-h}{f}$$

e [N/tex]
f [-]
h [-]

$$\Sigma_v = v(\dot{\varepsilon_v}, \varepsilon_v) = W_2(\varepsilon_v) \cdot \sinh^{-1}\left(\frac{\dot{\varepsilon_v}}{W_1}\right)$$

W_1 (s^{-1})

$$W_2(\varepsilon_v) = a_{w2} \cdot \varepsilon_v^{\alpha} + b_{w2}$$

α [-]
a_{w2} [N/
b_{w2} [N/

POLYAMOOR law: identification method

- Parameters identification from a multi-relaxation test

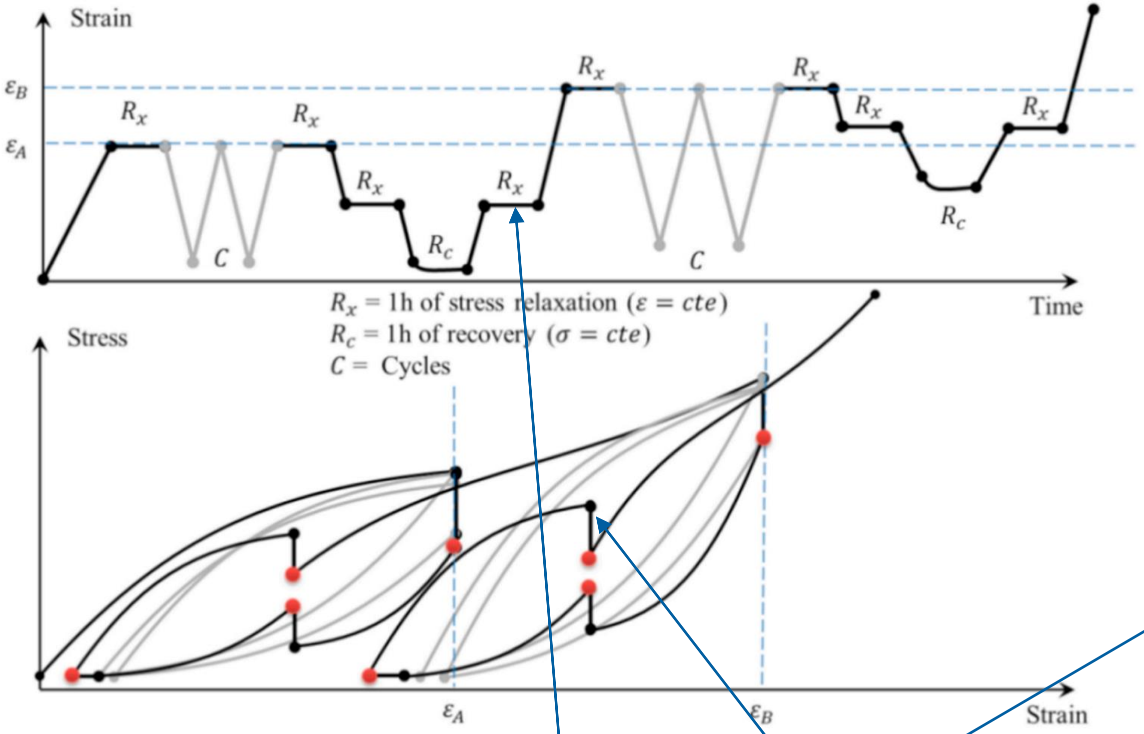

Relaxation plateaus

L.Civier, Y.Chevillotte, C.Bain, G.Bles, P.Davies, Y.Marco, **Visco-elasto-plastic characterization and modeling of a wet polyamide laid-strand sub-rope for floating offshore wind turbine moorings, Ocean Engineering (2024)**

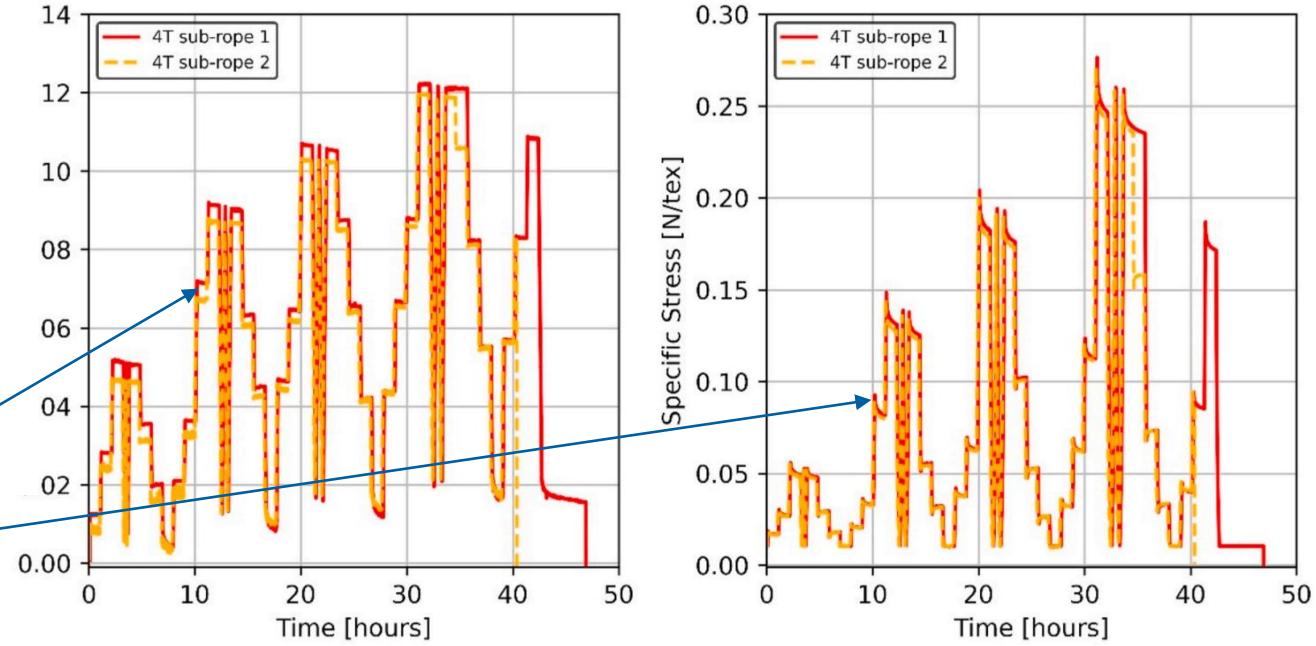

POLYAMOOR: Test set ups needed

Law identified usind a multi-relaxations test procedure:

- Strain interval: 0 to 12%
- Strain rate: 10^{-5} s-1

Figure: Servotest machine used in the laboratory of ENSTA Bretagne [1]

Small scales

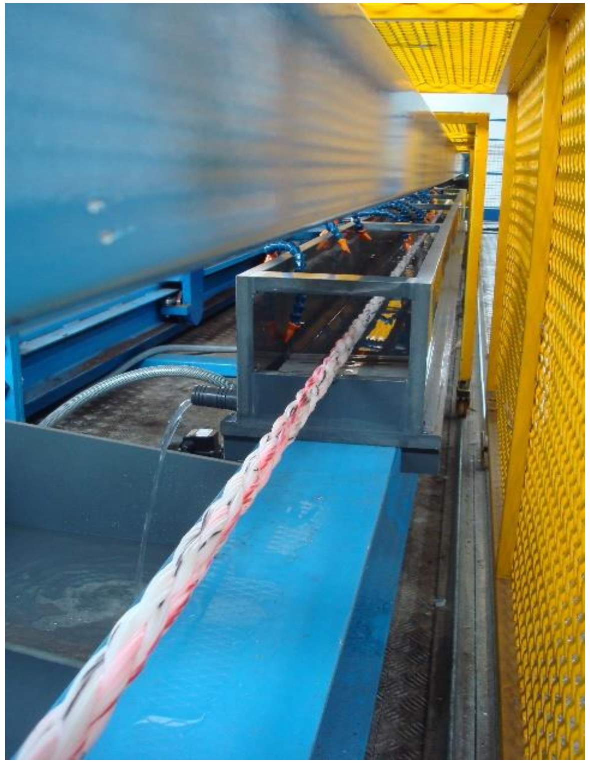

Figure: Ifremer test bench

Middle and high scales

Figure: BEXCO test bench

High scales

First validation of the law on small scales/middle scales

- Law POLYAMOOR is accurate for tests of:
  - Short creep
  - Multi-relaxation
  - Multi-creep
  - Stochastic loading

Characteristic times:
few secondes to few hours

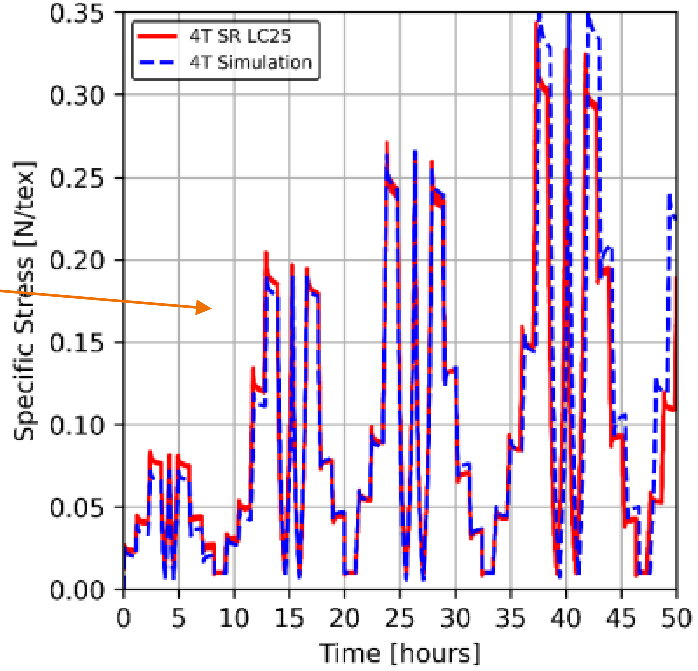

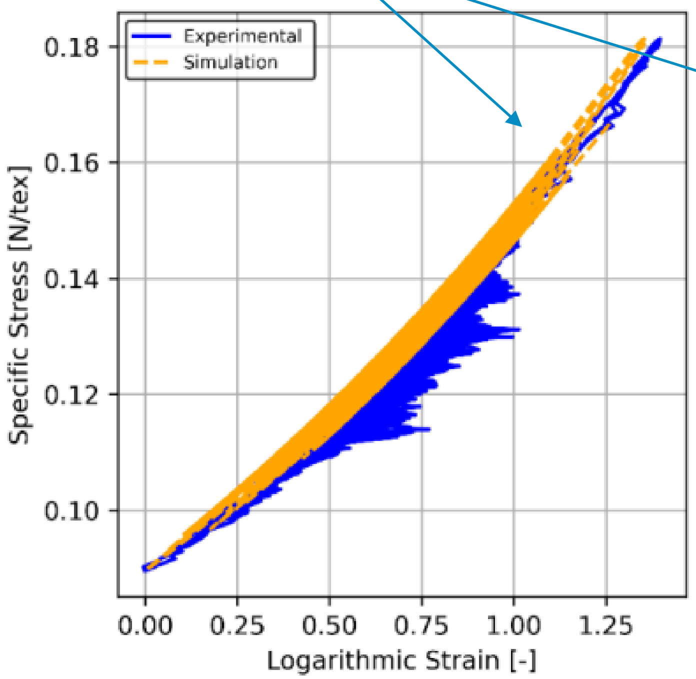

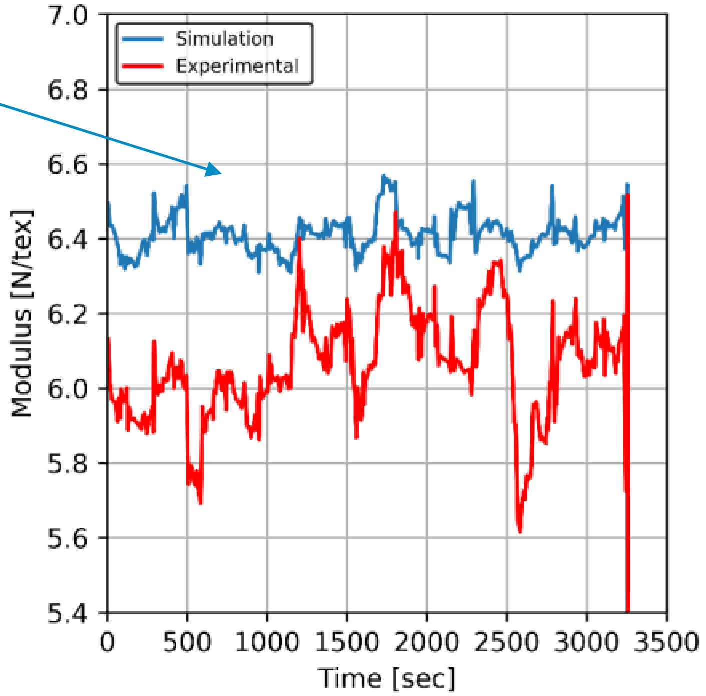

First validation of the law on small scales/middle scales

FRANCE ENERGIES MARINES

- Law POLYAMOOR is not accurate for tests of:
  - Long-term creep
  - Fatigue, above a certain number of cycles

Characteristic times: few hours to months

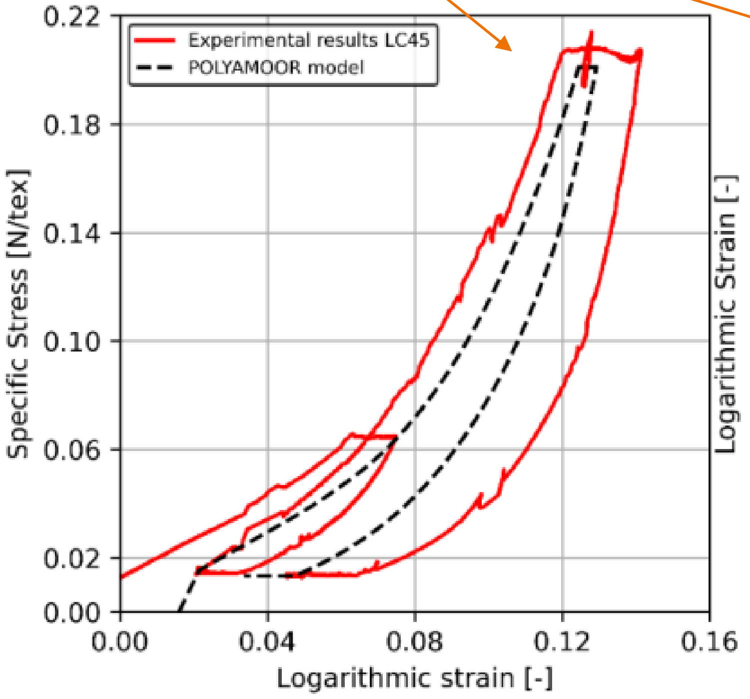

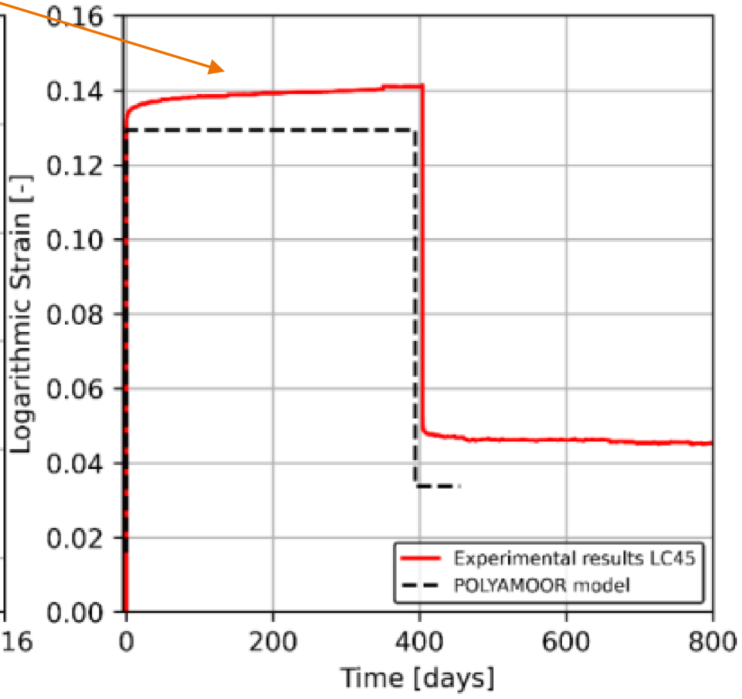

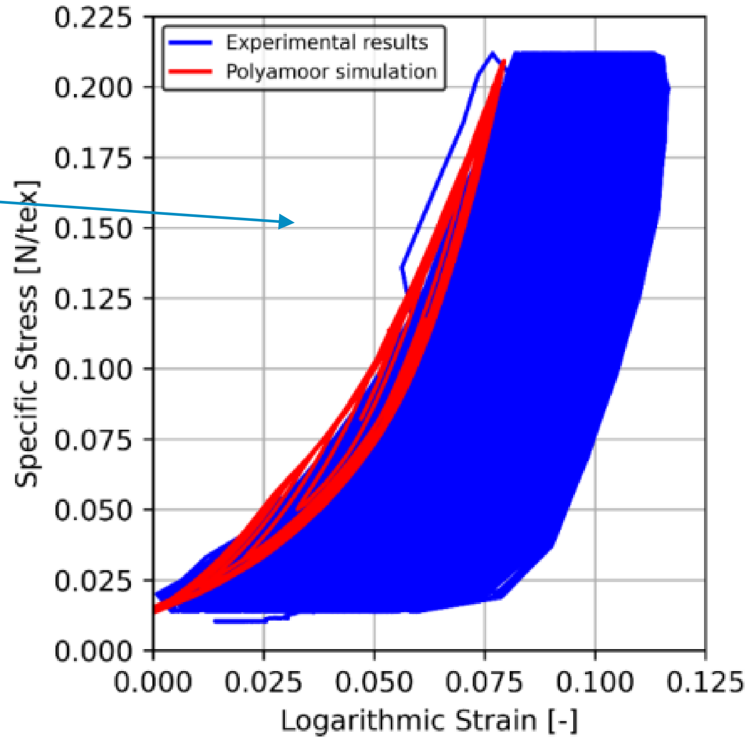

Questionable: only one test !

Comparison with at sea trials

POLYAMOOR behavior law → Law parameters identification process → Validation of the law in lab → Monitoring at sea

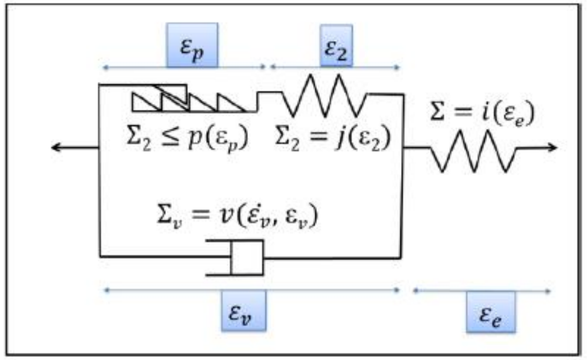

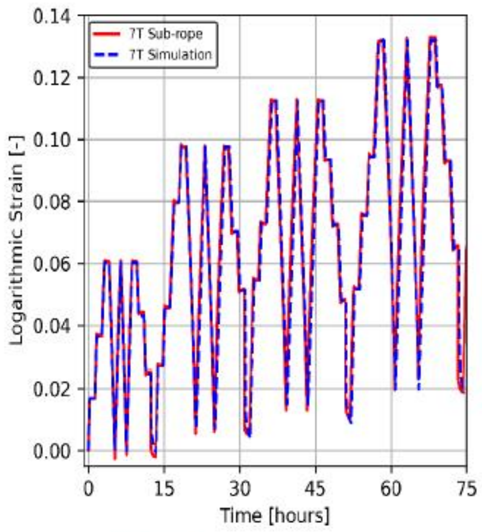

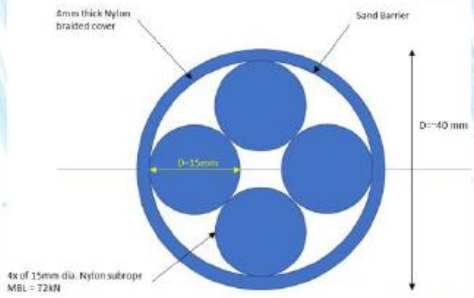

At sea-trials: buoy moored with experimental set up

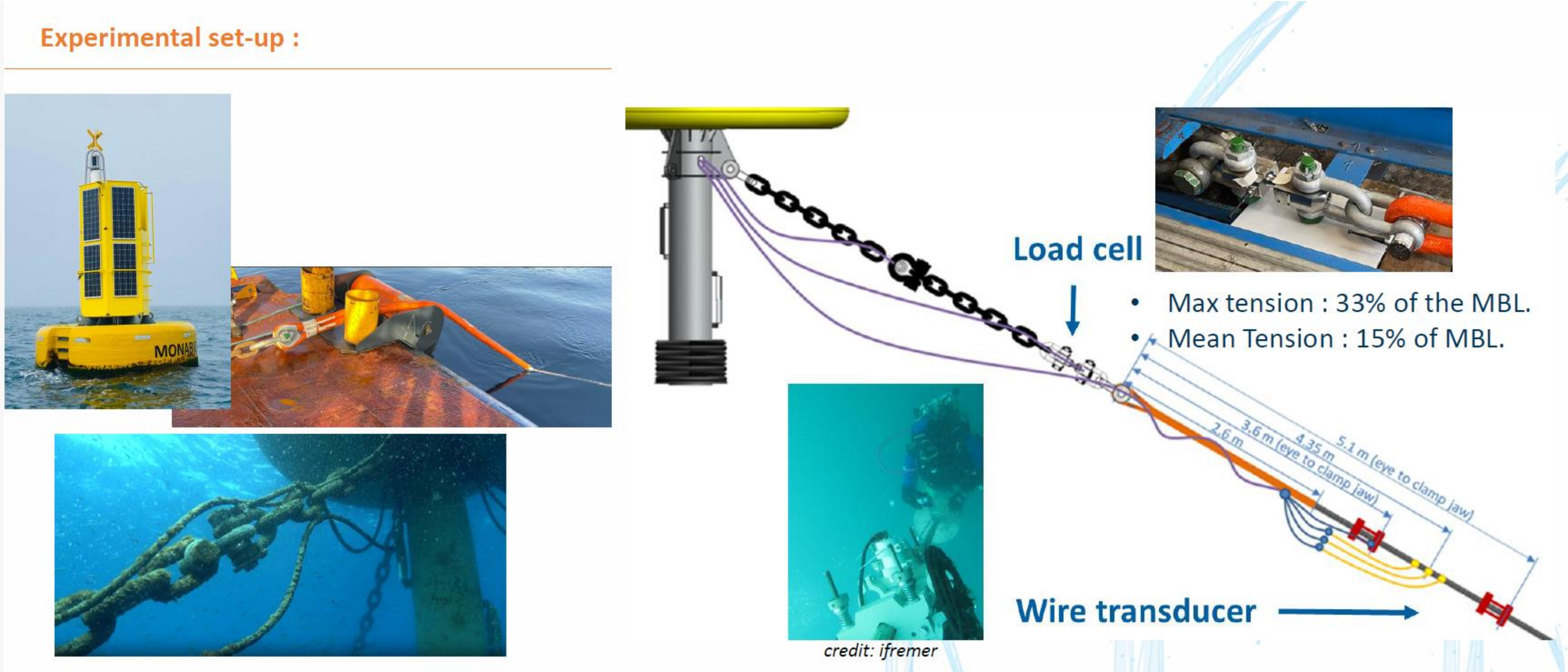

Measurements obtained

Long term measurement dataset

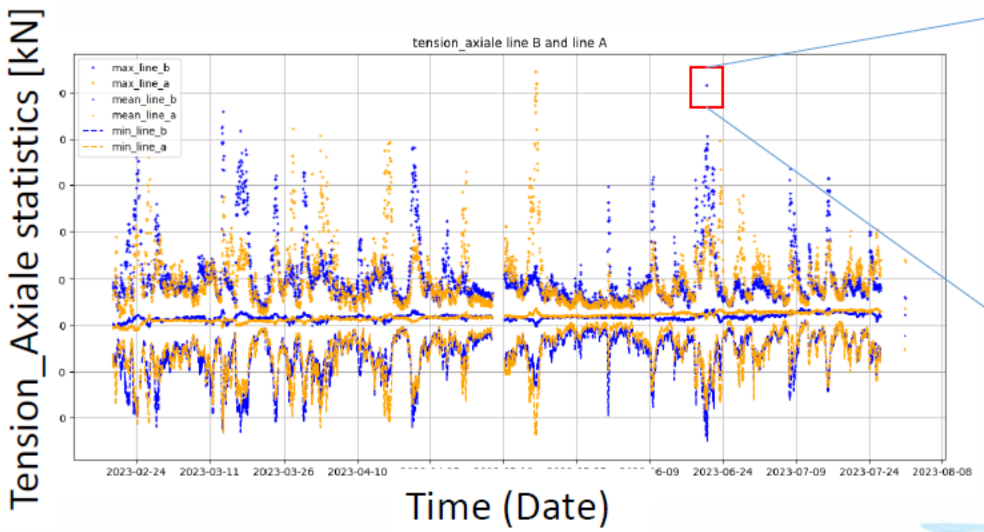

- **Mean tension has been almost stable.**
- Maybe sensor drift, to be checked at sensor recalibration.
- Several high load events before the selected one.

Dataset Available with measurements from Feb. 23 to Aug. 23

Zoom on 20/06/2023

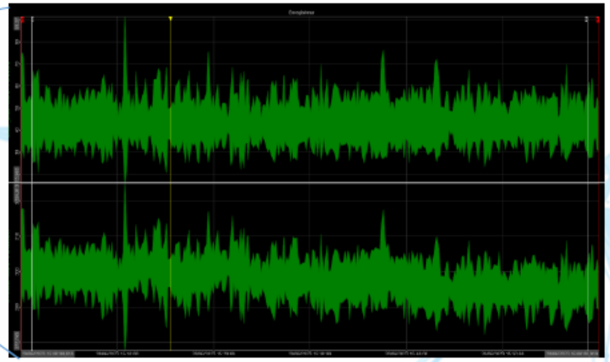

Tensions and elongation time series

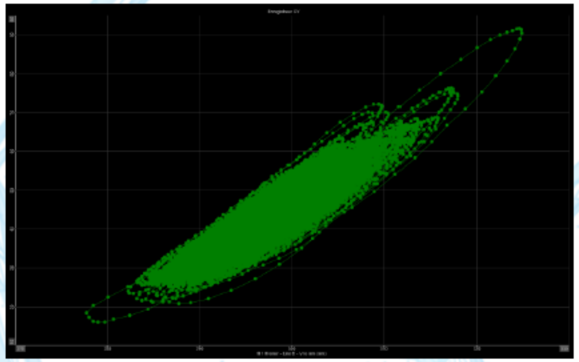

Elongation vs. tension

- Sensors are time synchronized
- Sensor data @ 10Hz

Deeplines model set up

Deeplines Model set-up

- Pure traction test set-up.
- Impose of tension sensor recording @ 10Hz

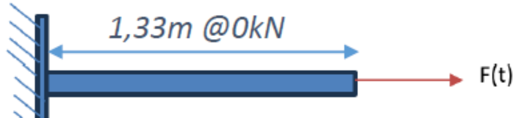

Model set-up illustration

Compare POLYAMOOR behavior law vs. dynamic stiffness law

	POLYAMOOR behavior law	Dynamic stiffness
Constant parameters for all load cases	✓	⊗
Available in most commercial software	⊗	✓ ⊗
Model during dynamic simulation	$T = f(\epsilon, \dot{\epsilon})$	$T = Kd(Tmean, Tamp) * \epsilon$
Model viscosity & plasticity	✓	⊗

Cross validation of model behavior laws & elongation sensor measures

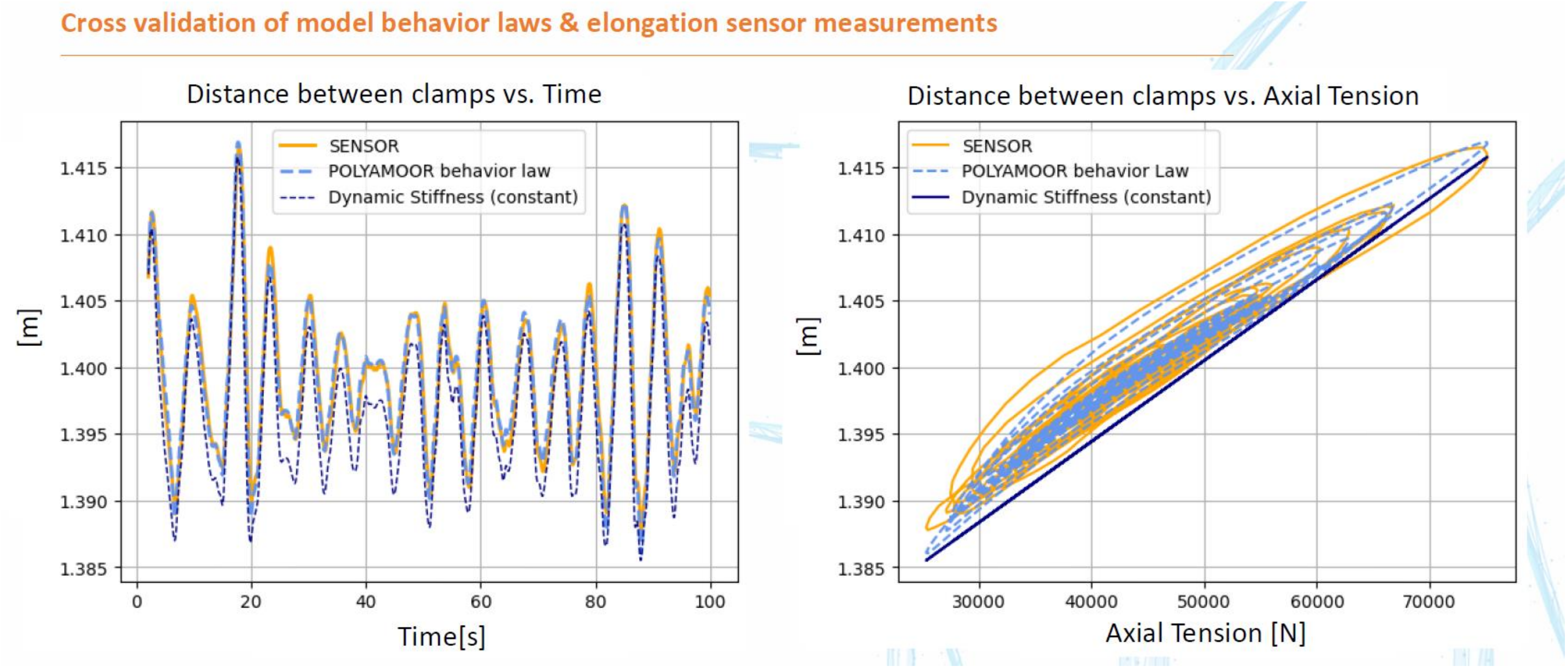

Used ropes campaign: bibliography

Experimental test performed on a laid polyamide rope after 18 month deployment in sea (WEC application).

Rope construction: 7 parallel-stranded sub-rope covered by a non-bearing-load cover and without filter cover

Experimental test campaign performed on the aged rope:

- Quantification of the marine growth: weight and diameter measurements
- Aged sub-rope and yarn assemblies subjected to: harmonic loading, tension fatigue,

tensile test to failure

- SEM images
- Yarn-on-yarn abrasion test

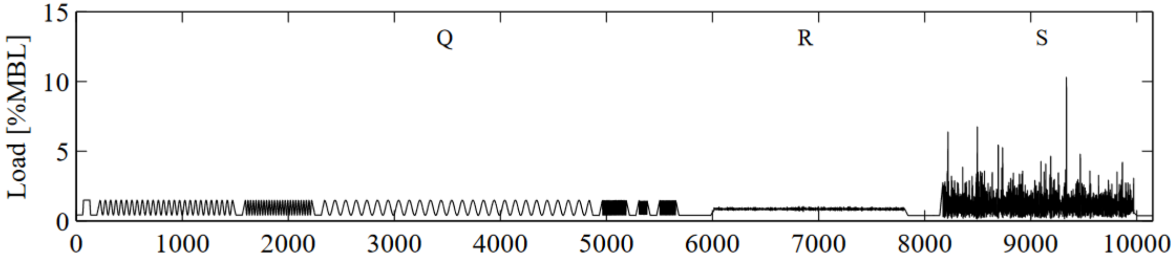

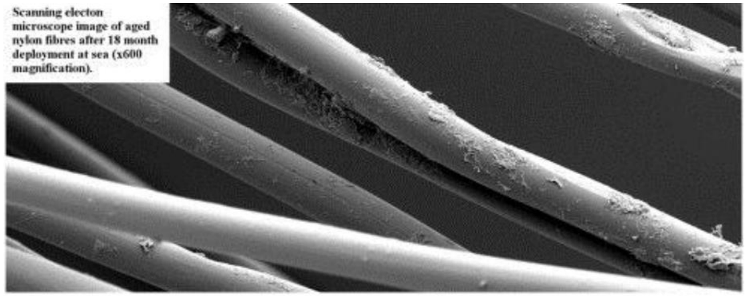

Scanning electon microscope image of aged nylon fibres after 18 month deployment at sea (x600 magnification).

Conclusions:

- Aged yarns showed lower performances
- Due to two main damage mechanisms: abrasion wear between outer yarns and jacket due to sediment and mussel infiltration (external abrasion/damage) and fibre-on-fibre wear during tension fatigue

Weller, S.D., P. Davies, A.W. Vickers, et L. Johanning. « Synthetic Rope Responses in the Context of Load History: The Influence of Aging ». Ocean Engineering 96 (mars 2015): 192-204. https://doi.org/10.1016/j.oceaneng.2014.12.013.

Perspectives: BAMOS and J.Laurent PhD

Enhanced 1D behavior law for PA rope and scale effect

- Identification of the viscous parameters on the MONAMOOR long-term creep data.
- Identification of the whole set of parameters on longer-term multi-relaxation tests (2 or 3-hour-long plateaus instead of 1-hour currently)
- Tests and identification of the POLYAMOOR 1D law on higher MBL sub-rope (7T, 25T, 45T)

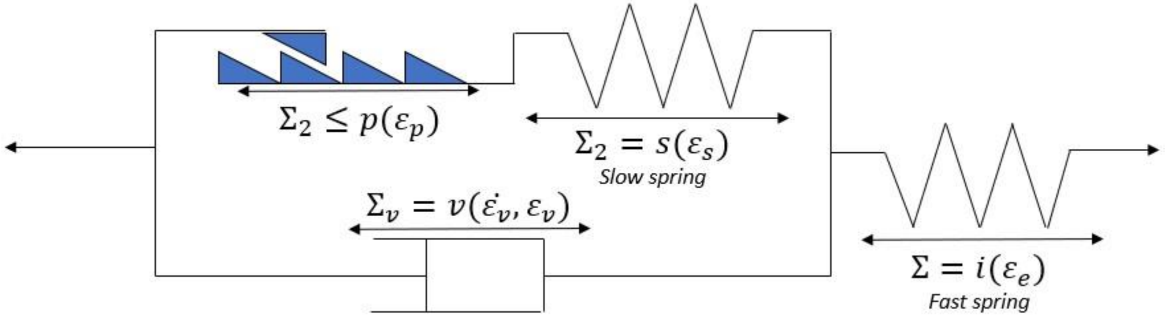

Table of contents

Fatigue study: state of the art

Fatigue → degradation and failure induced by repeated loading
Key limitation for polyamide ropes

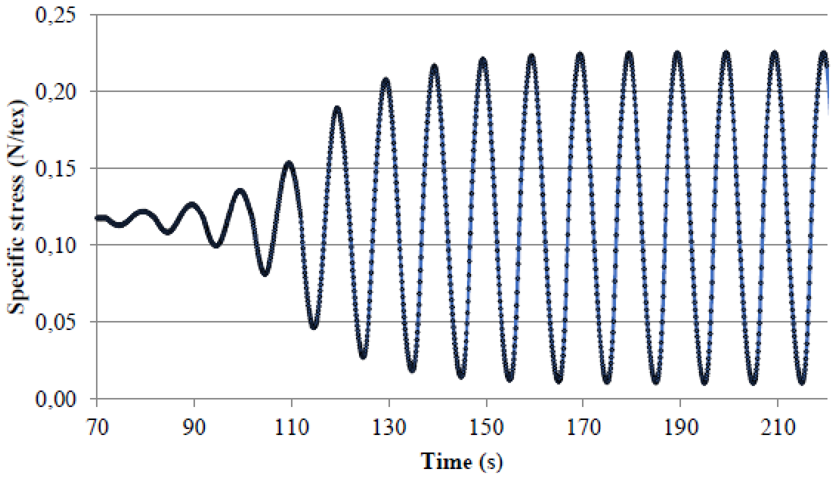

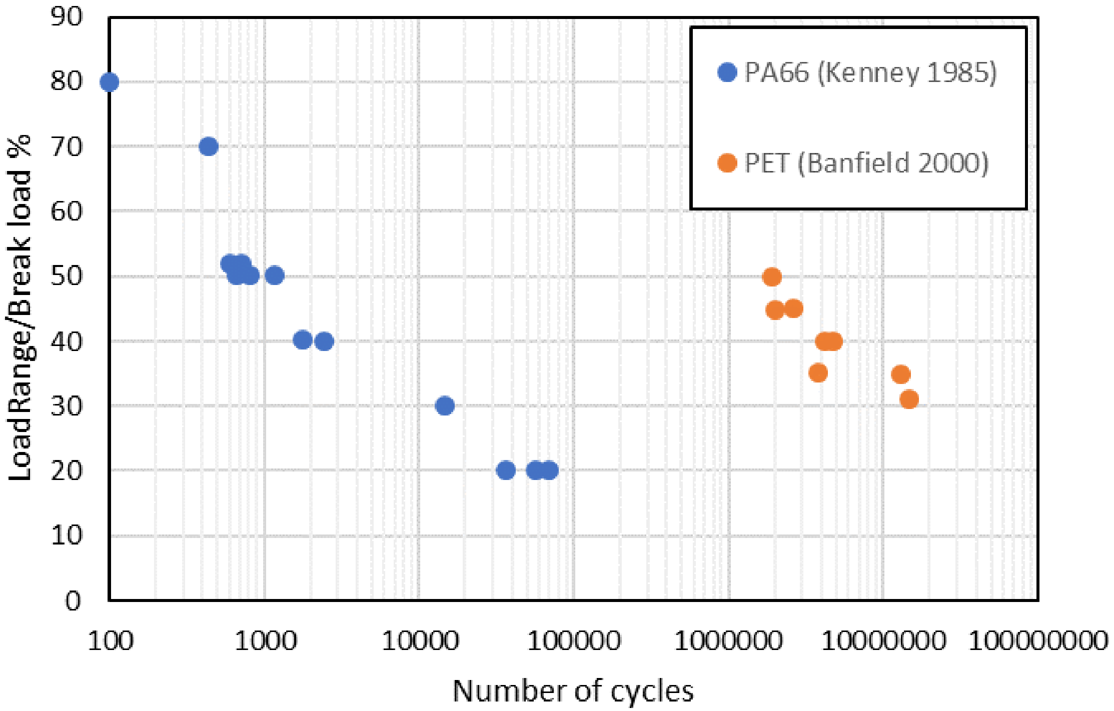

Fatigue study: state of the art

FRANCE ENERGIES MARINES

Fatigue → degradation and failure induced by repeated loading
Key limitation for polyamide ropes

What are the damage and failure mechanisms ?

- At the fibres scale (Herrera *et al*. 2004):
  - Creep
- At the strands and sub-ropes scale: (Parsey *et al. 1983*)
  - **Structural fatigue**
  - **Internal abrasion**

→ Evolution of the <u>construction</u> and <u>coating</u> to increase fatigue durability: **provide a suitable fatigue lifetime.**

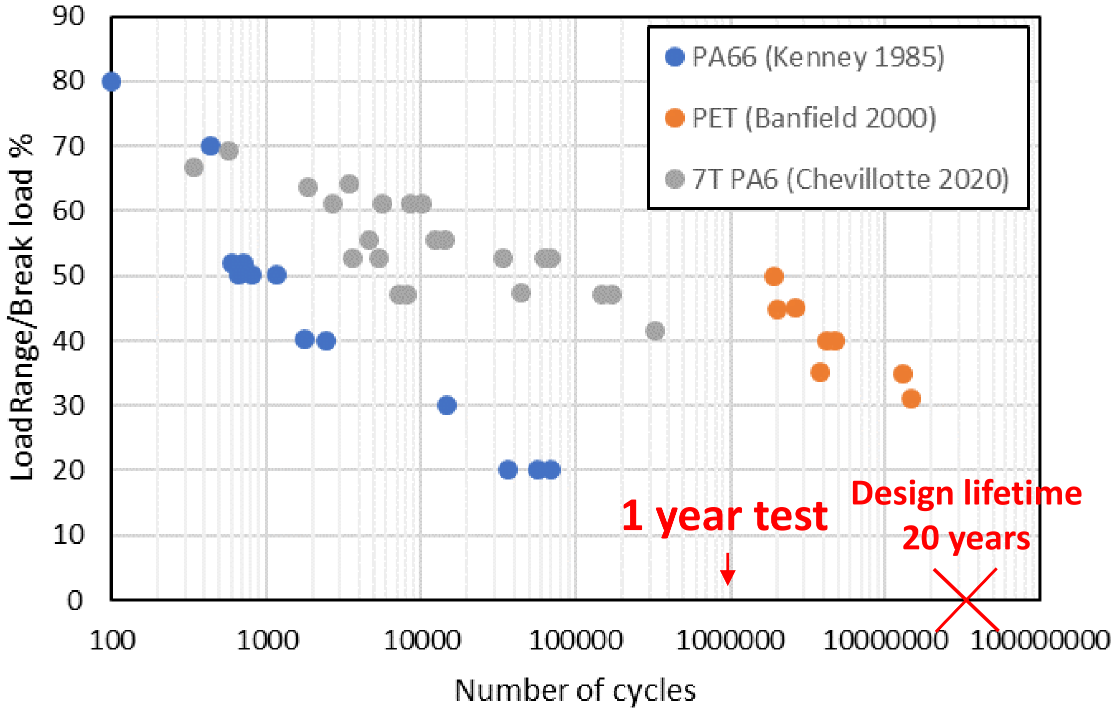

→ Better understand the construction impact on fatigue and perform screening of construction

→ Development of a model

Chevillotte *et al. 2020*

Experimental set up

Fatigue campaign:

- Frequency of 0.1 Hz
- Between a fixed minima at 2 %MBL and varying maximal (R ratio close to 0)
- Fatigue test stops at the failure of the specimen

Study of the laboratory scale: 4T

900 mm long sample with two splices manually made

Immersion of the sub-rope at least 24h before the test

Rope maintained wet during the test

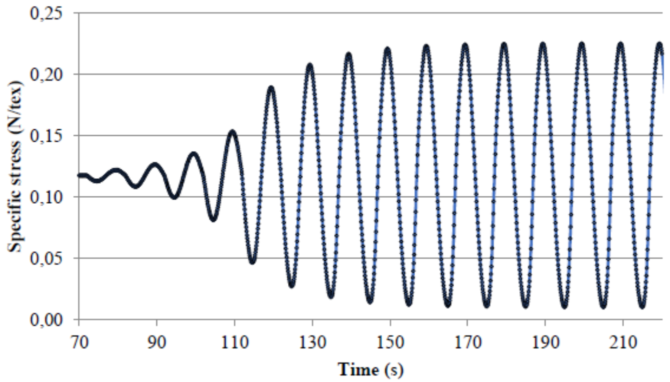

Watering system

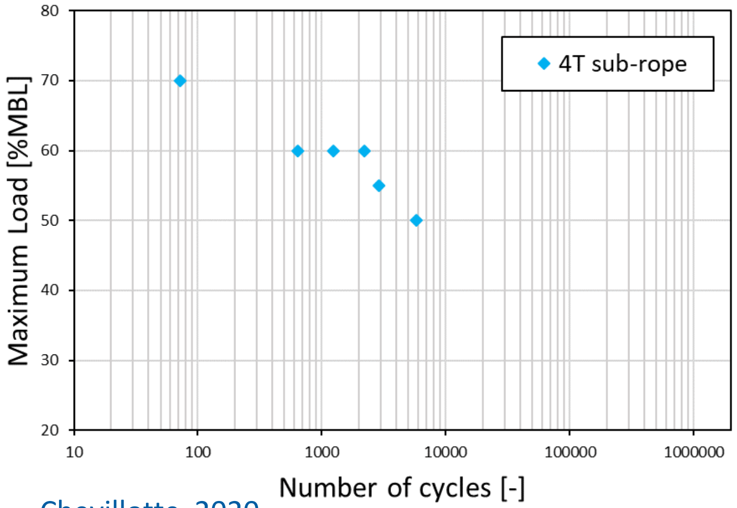

Chevillotte. 2020.

March-may 2024 fatigue campaign

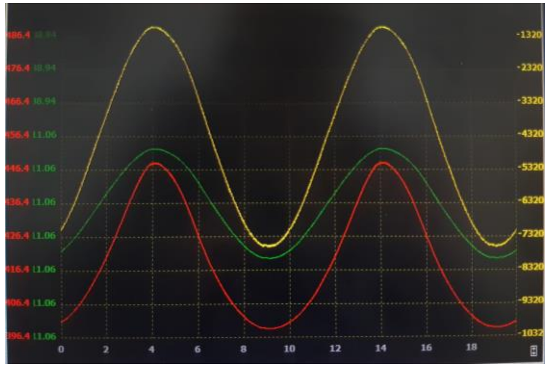

0,1 Hz

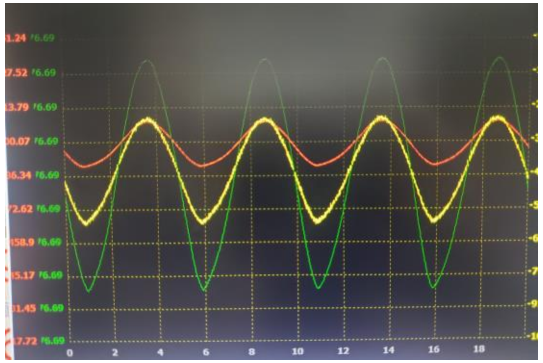

0,2 Hz

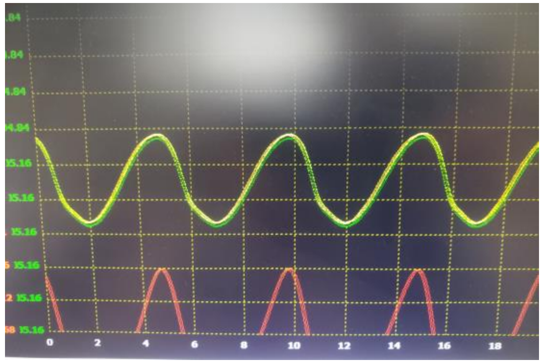

0,2 Hz

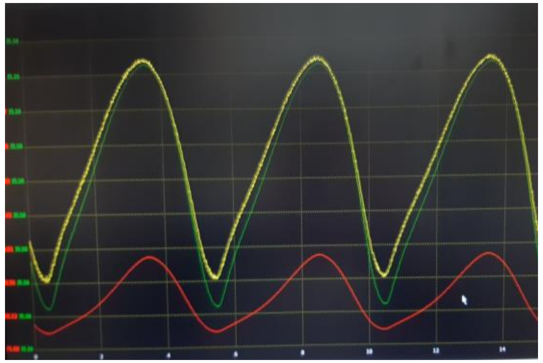

0,2 Hz

Not possible to increase frequency, we keep 0,1 Hz.

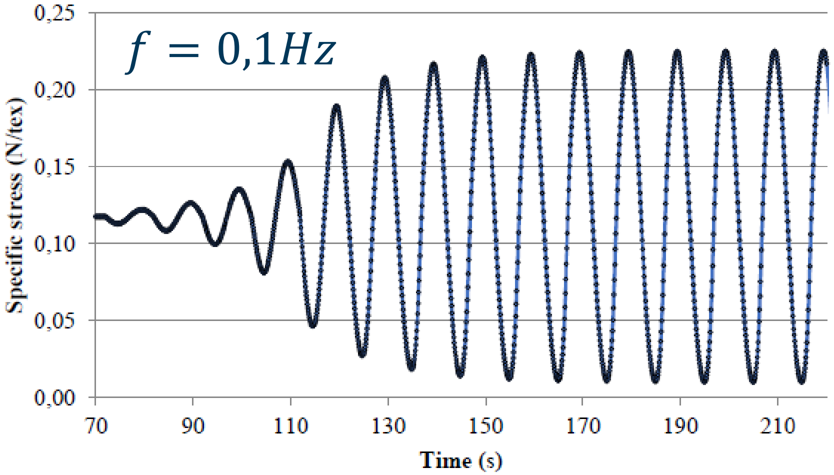

10 cycles to set-up the load amplitude value

Fatigue campaign

FRANCE ENERGIES MARINES

<u>*Our test campaign:*</u>

- 4T sub-rope
- R ratio close to zero
- Fmin fixed and varying Fmax

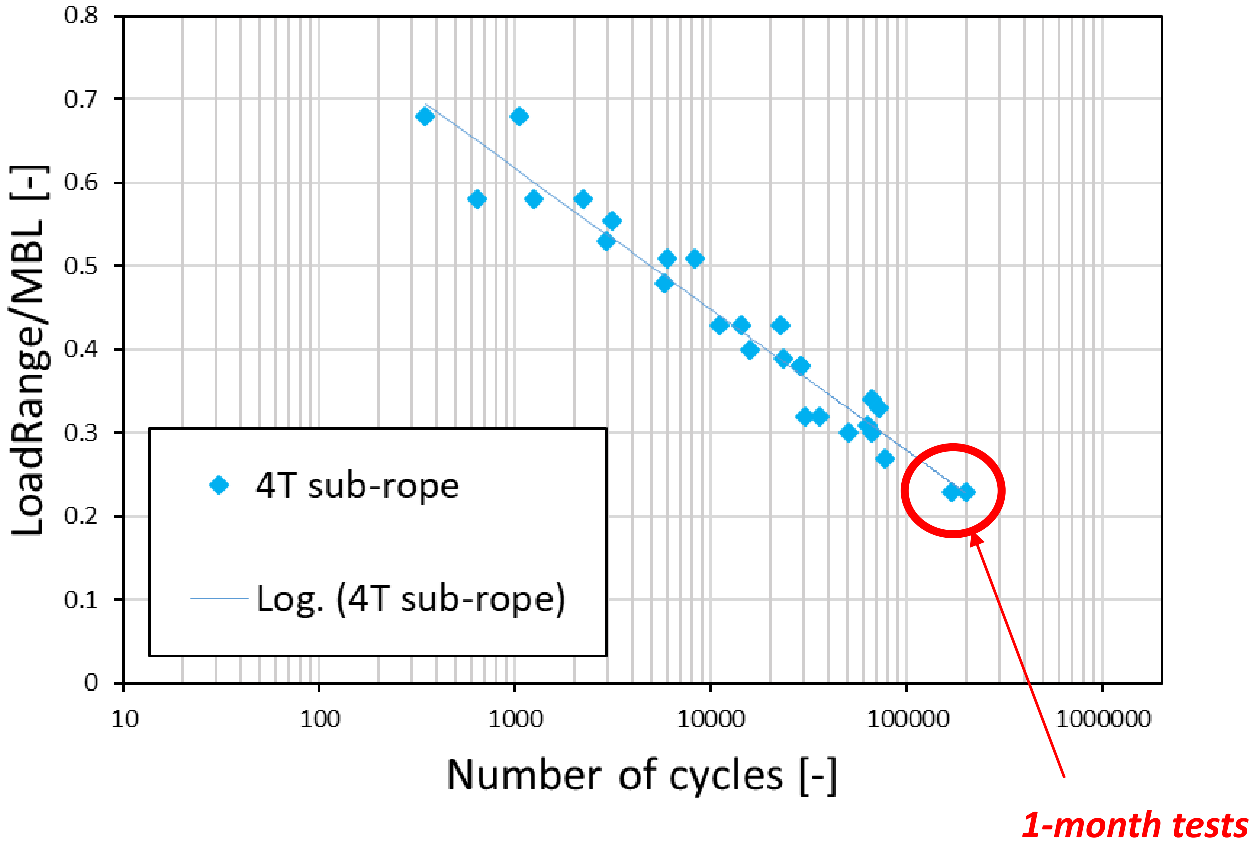

<u>*Conclusions:*</u>

- Linear trend observed for the 4T tested load ranges

Fatigue campaign

Our test campaign:

- 4T sub-rope
- R ratio close to zero
- Fmin fixed and varying Fmax

Chevillotte 2020:

- 7T sub-rope
- R ratio close to zero

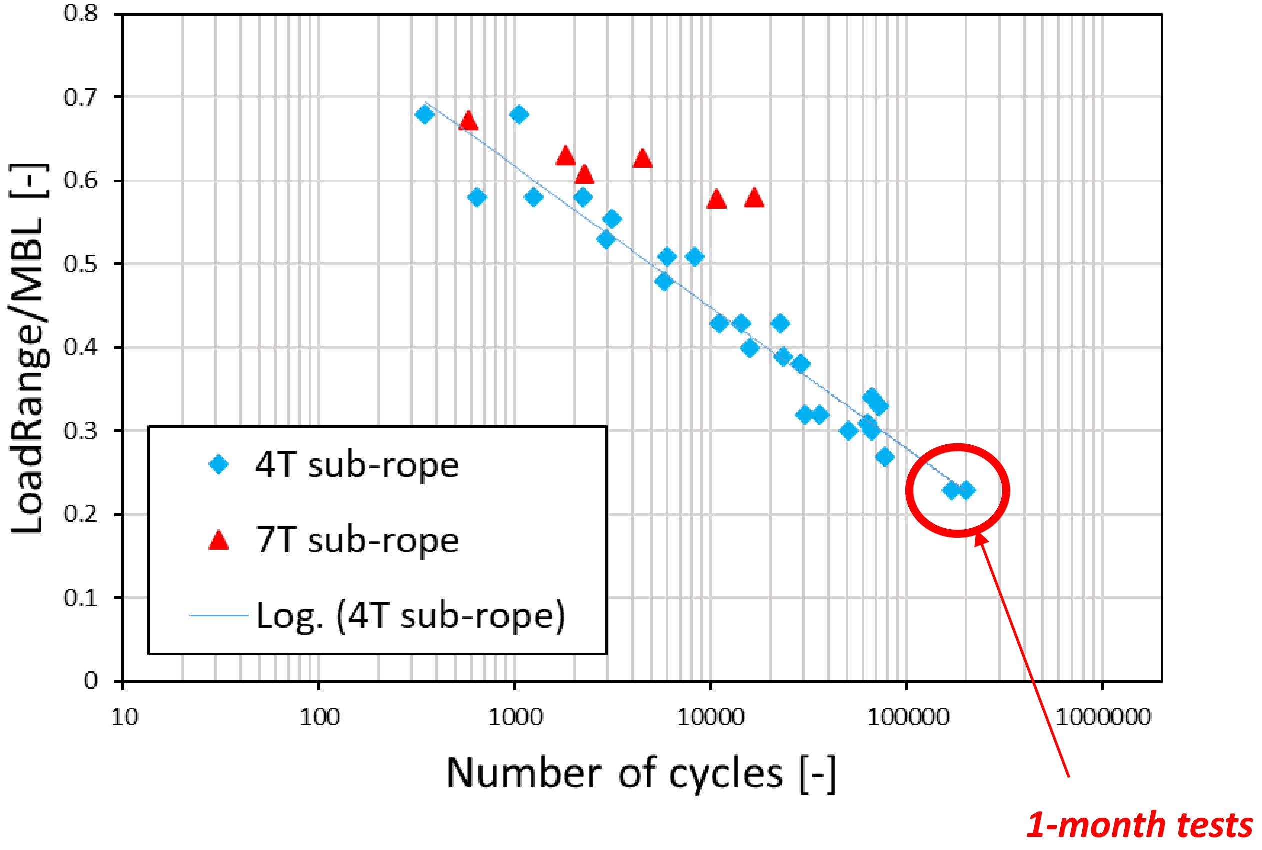

Conclusions:

- Linear trend observed on semi-log plot for the 4T tested load ranges
- The smaller lay-length impacts the fatigue lifetime
- The results obtained with the 4T scale sub-rope are close to the results for more realistic constructions

Fatigue campaign

<u>*Our test campaign:*</u>
- 4T sub-rope
- R ratio close to zero
- Fmin fixed and varying Fmax

<u>*Chevillotte 2020:*</u>
- 7T sub-rope
- R ratio close to zero

<u>*Banfield 2017:*</u>
- Twisted polyamide sub-ropes with two constructions.
- R ratio varying between 0.3 and 0.5

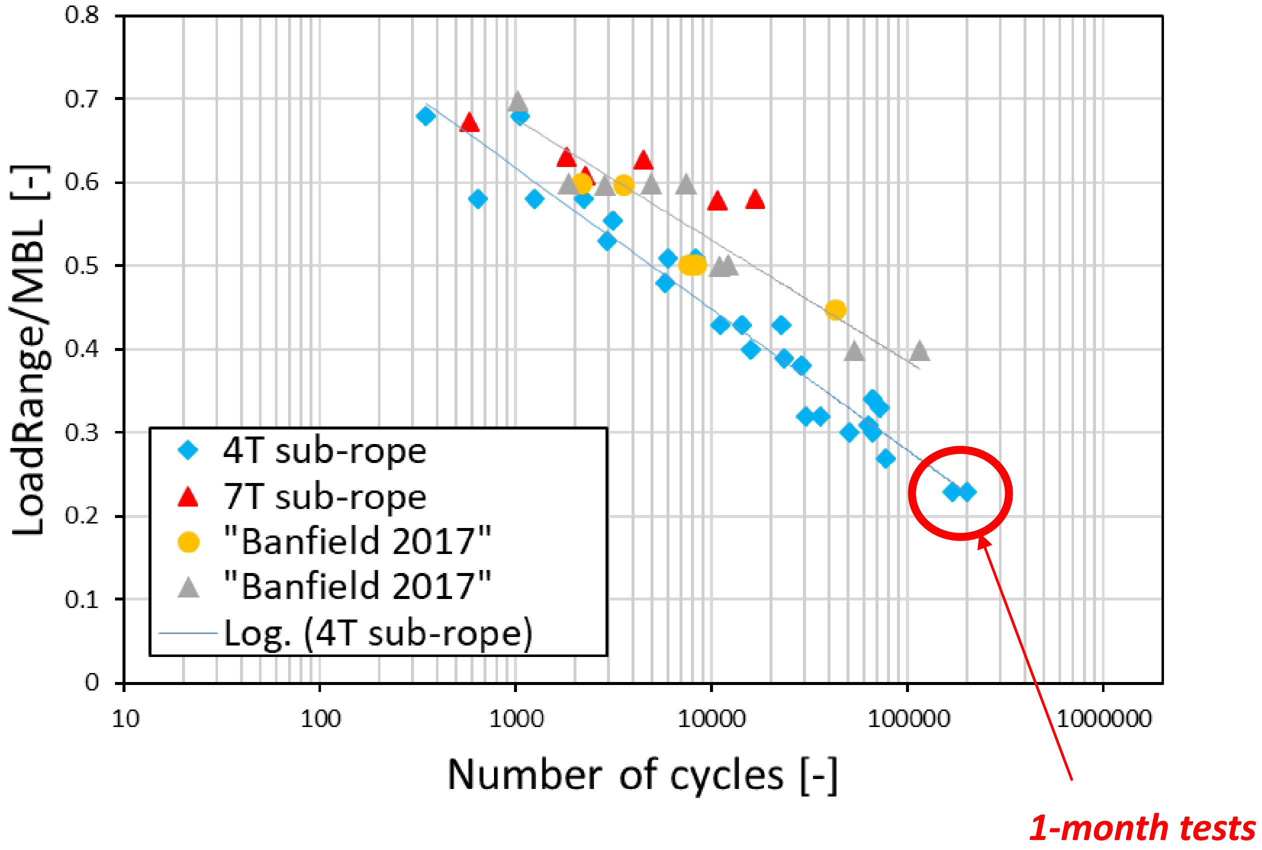

<u>*Conclusions:*</u>
- Linear trend observed for the 4T tested load ranges
- The smaller lay-length impacts the fatigue lifetime
- The results obtained with the 4T scale sub-rope are close to the results for more realistic constructions

Fatigue campaign: on-going project

70%MBL 49%MBL 20%MBL

Failure in the eye's splice.
Conservative result

Interrumpted test.
Conservative result

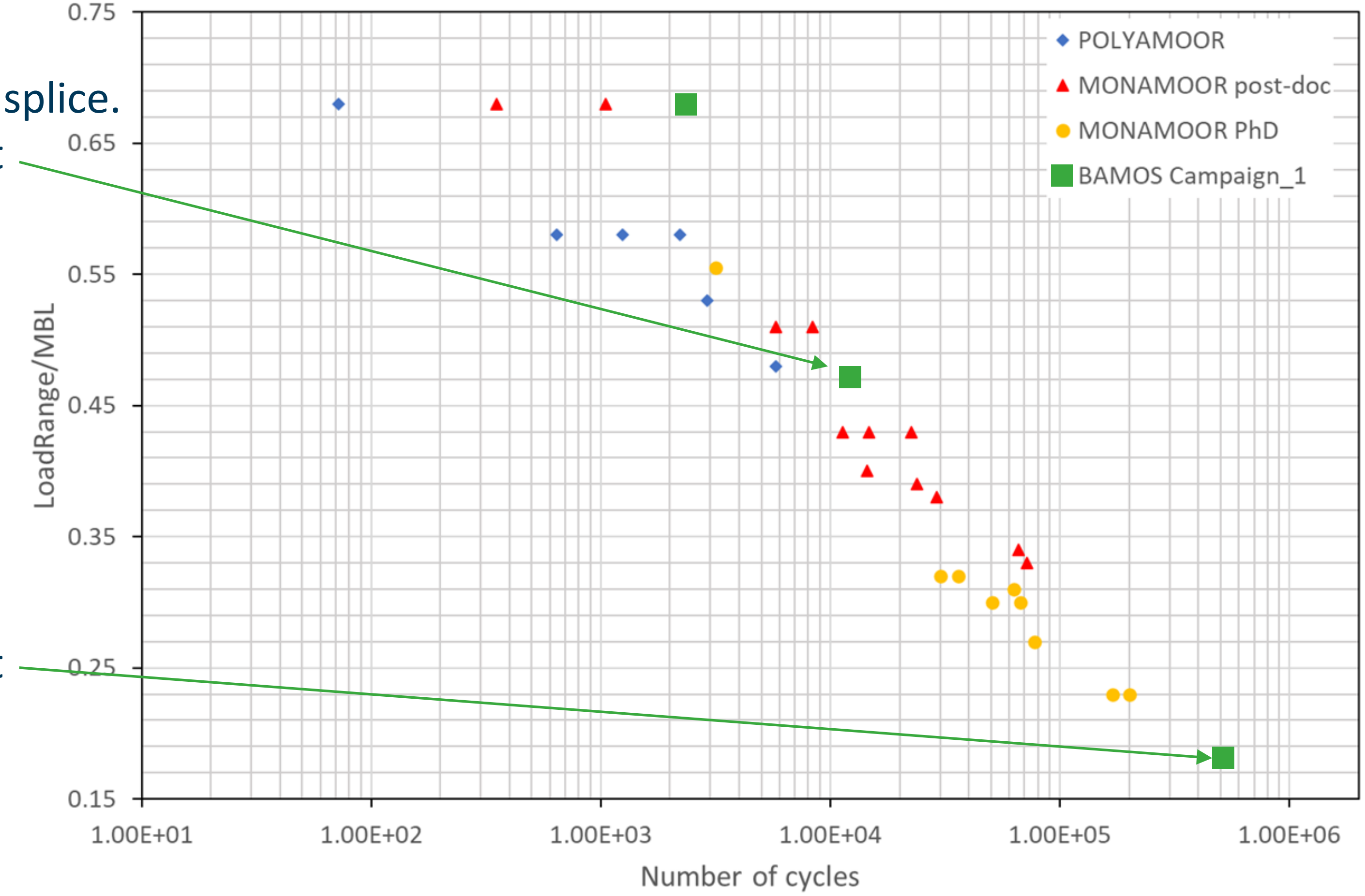

Tomography study on aged rope

Studied specimens

Sample after 29 %MBL fatigue test

Virgin sample

Experimental set-up

- Polyacetal container
- One lay pitch can be scanned
- Tension 400 N

Tomography: experimental set up

FRANCE ENERGIES MARINES

Tomography at CRT Morlaix.

Higher resolution available: 20 µm.

3 scans with 2200 pictures per scan

Total time of a tomography: 45 minutes

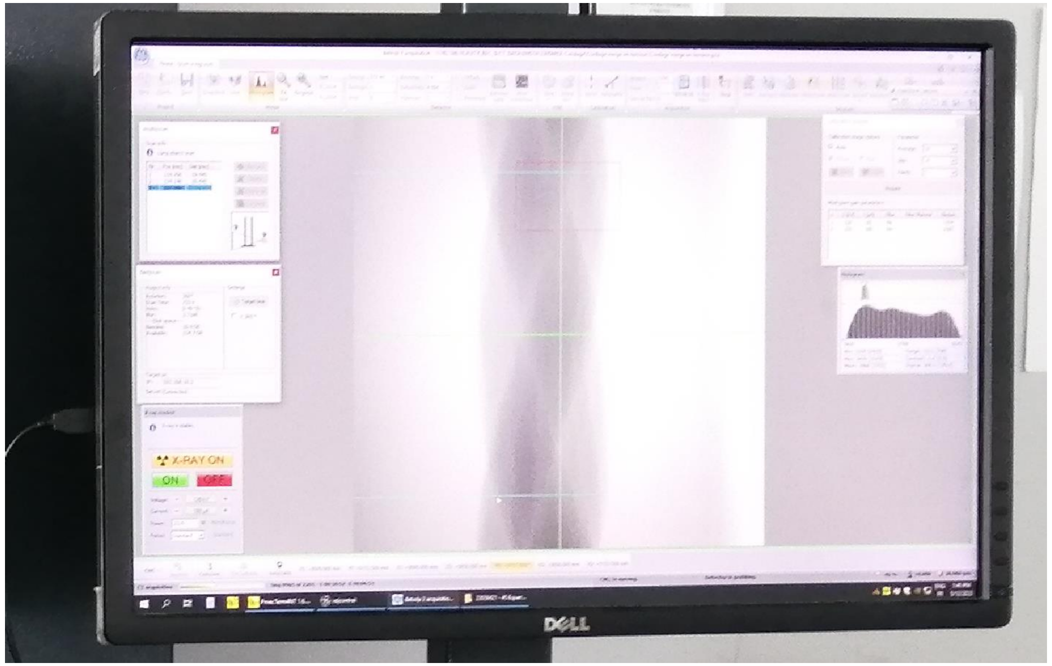

Tomography results: virgin/aged

Higher resolution available: 20 µm.

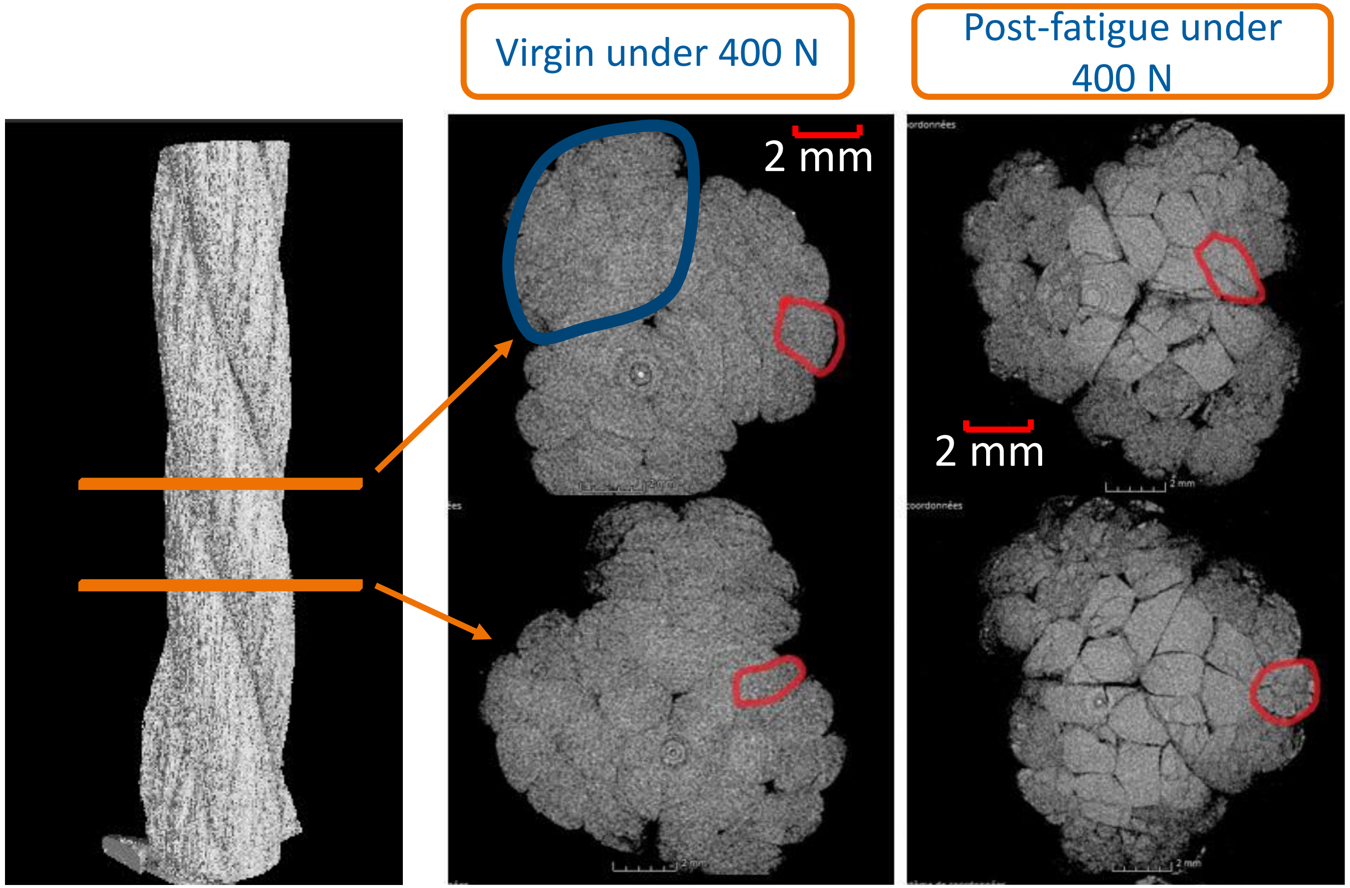

<u>Observations on the post-fatigue sample:</u>

- Gradient of compaction inside the sub-rope
- Rope-yarns shape very angular
- Contact area very visible

Tomography results: virgin/aged

No tension

Virgin under 400 N

Post-fatigue under 400 N

1 strand: 10 rope-yarns

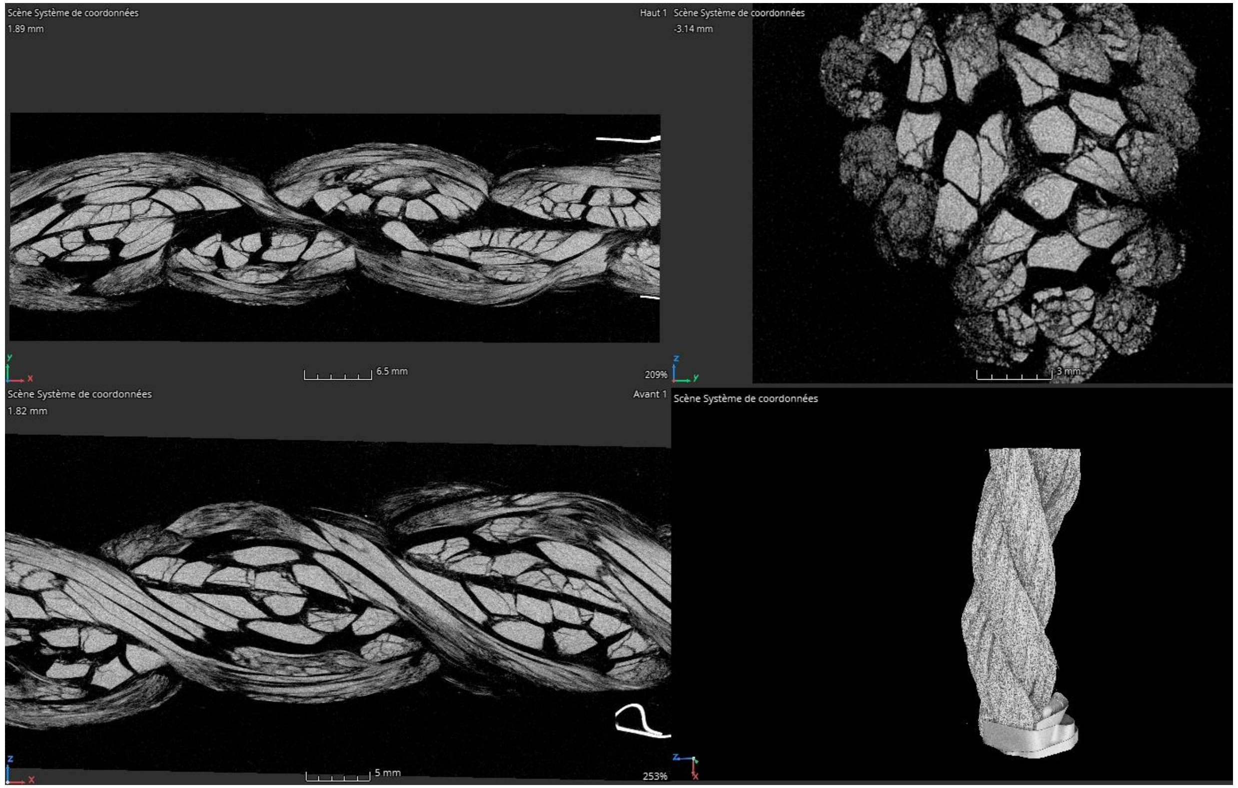

SEM results aged/virgin

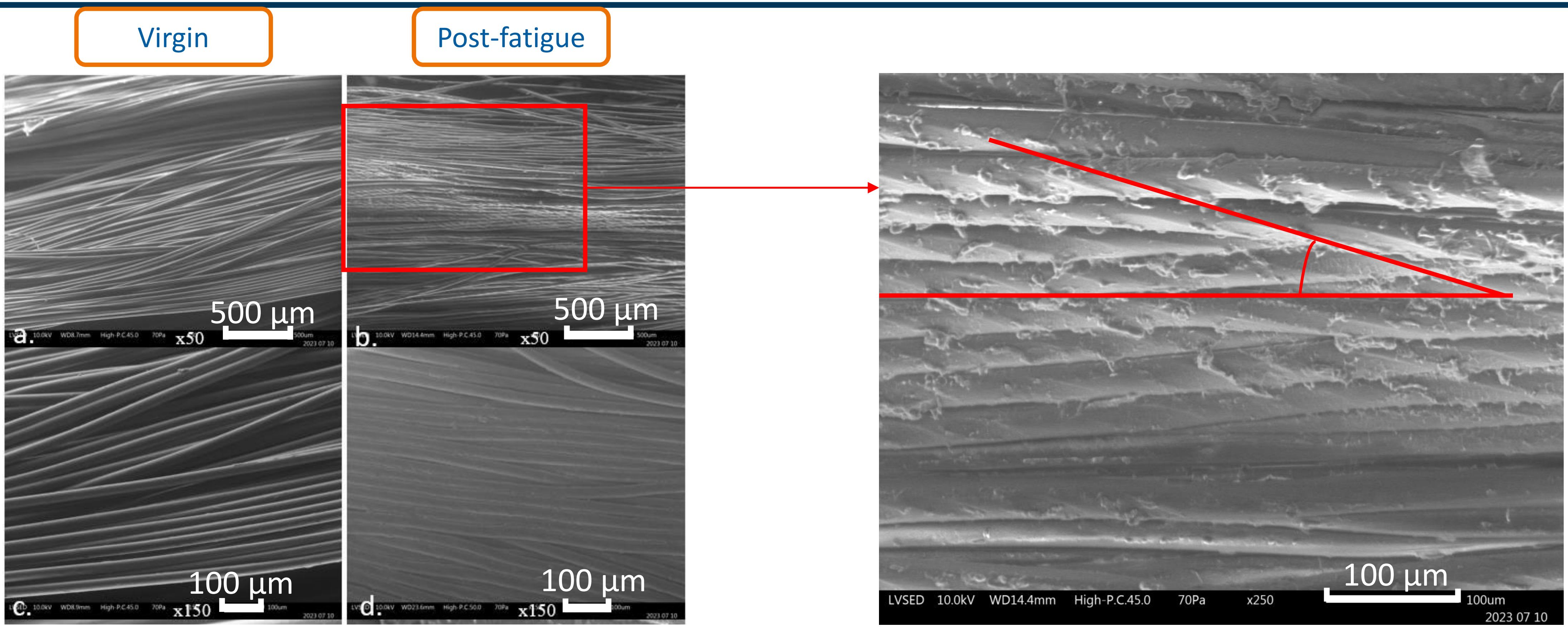

Observations on the post-fatigue sample:

- The filaments are more compacted and aligned

Observations on the zoom:

- Marks are due to the friction with the fibres in contact
- Friction coefficient will depend on the direction of the fibres

Fatigue study: conclusion and perspectives

Fatigue:

- S-N curve extended to 10^5 cycles on 4T sub-ropes
- The 4T construction is interesting to investigate fatigue: conservative and easier to study

Damage analysis:

- New state and organisation of the material at the rope-yarns scale:
  - More compact
  - Fibres more aligned
- The rope-yarns are sharper

How to speed-up the characterization of the fatigue curve ?

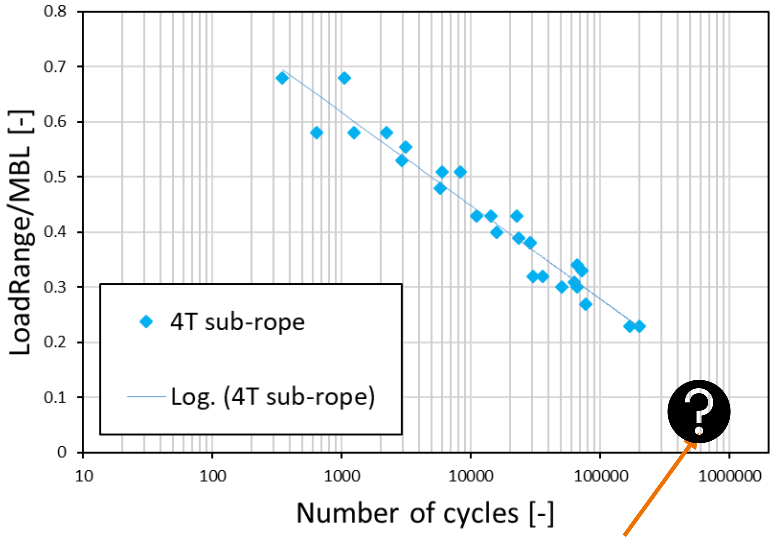

Self-heating for fast fatigue prediction

Additional study and perspectives: self-heating method

The self-heating method applied on sub-rope

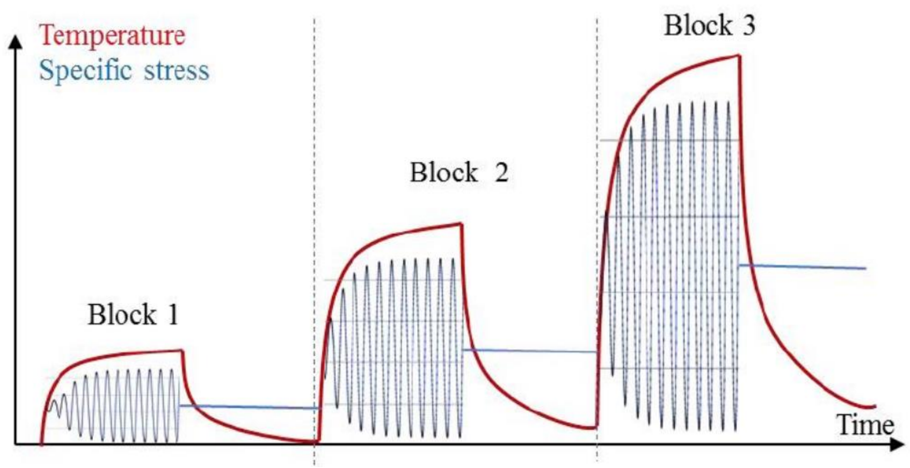

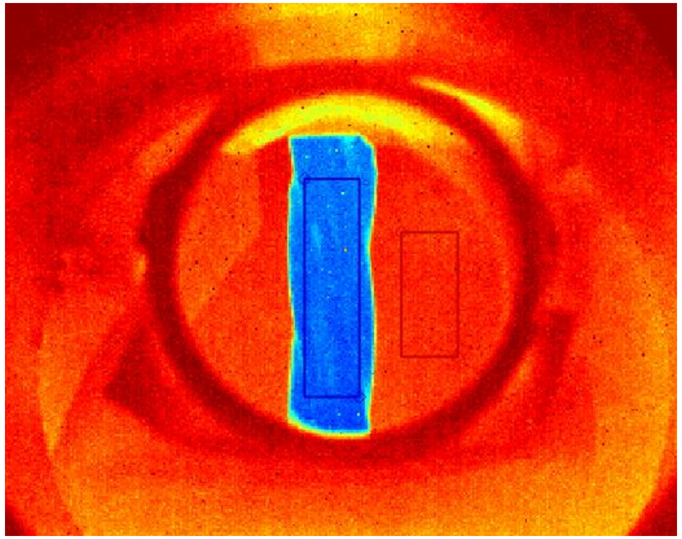

Image from Célénos software (Le Saux, V. (2023))

Several phenomena:

- Thermo-elastic coupling
- Inherent elevation of temperature due to potential damaging mechanisms

The global dissipation per cycle:

$$\Delta^* = \frac{\overline{\theta_{MAX}}}{f_r \times \tau_d}$$

Motivations:

- Link mechanisms and energy conversion to **damage and failure scenarios**
- Understand the **dissipation mechanisms**: $\Delta^*_{material} + \Delta^*_{friction}$

The self-heating method applied on sub-rope

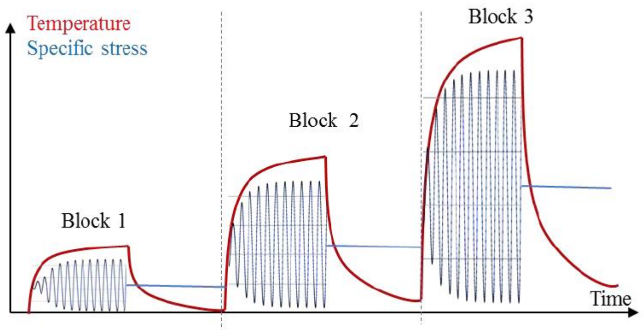

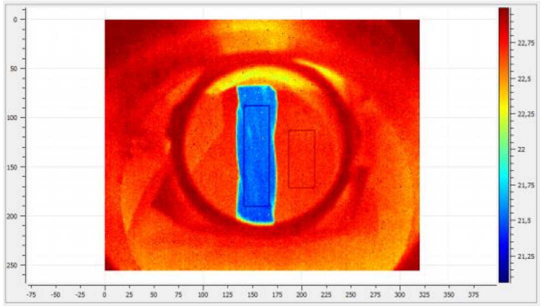

The global dissipation per cycle:

$$\Delta^* = \frac{\overline{\theta_{MAX}}}{f_r \times \tau_d}$$

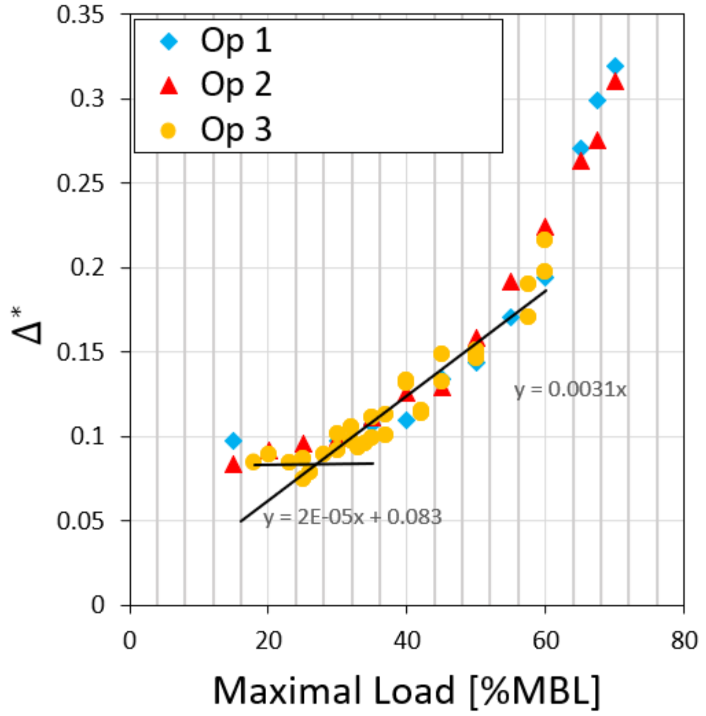

Use of an energy criteria to predict fatigue life:

$$\Delta^* N^b = C$$

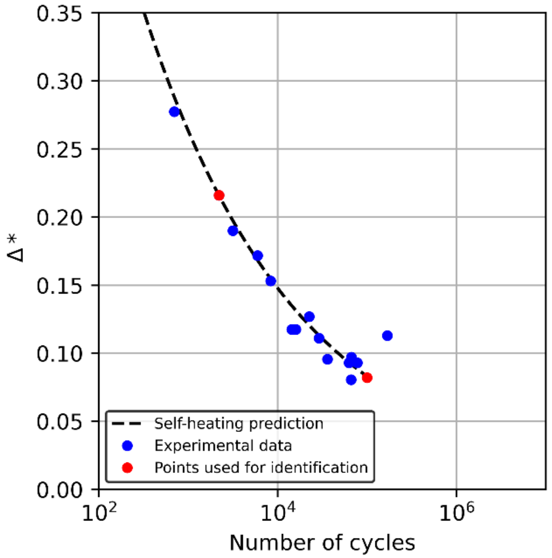

Mechanisms and energy conversion ↔ Damage and failure scenarios

The self-heating method applied on sub-rope

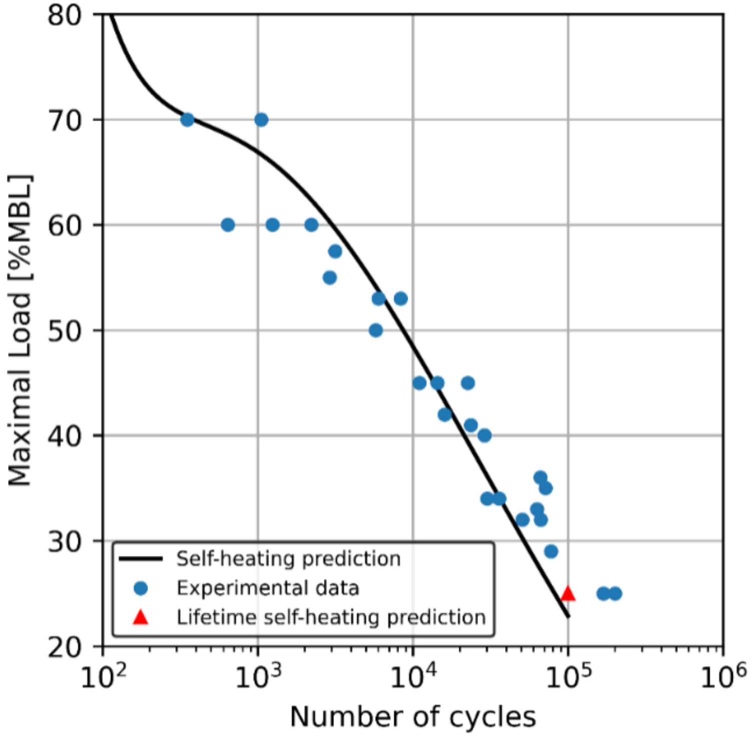

Obtention of a fatigue curve based on an energy criteria

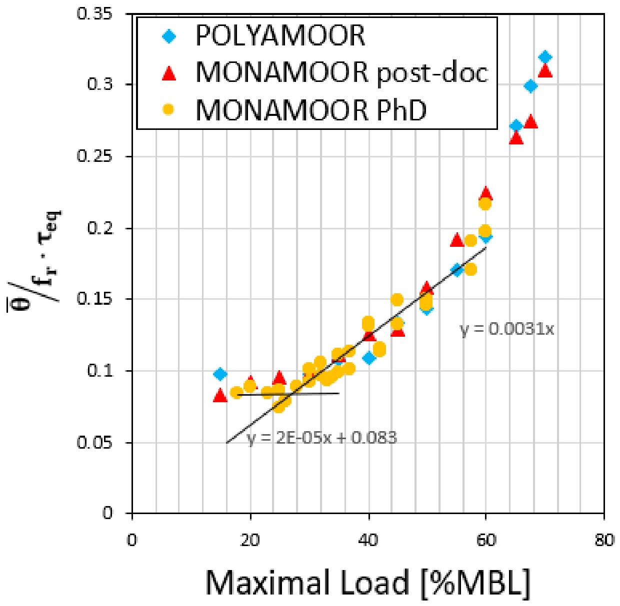

New graphical determination of regime

Need to overcome the graphical approach

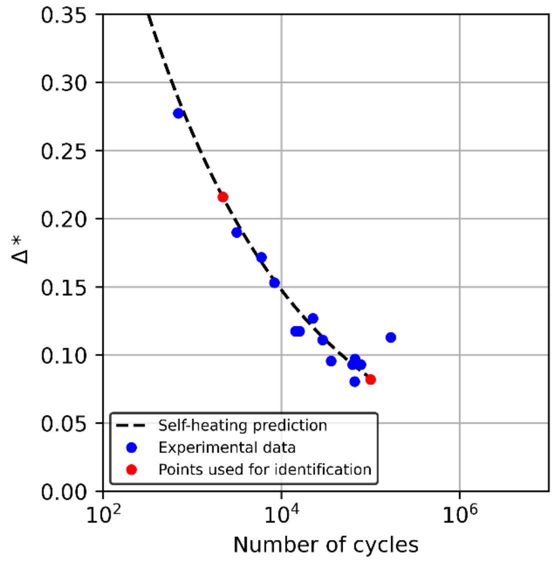

Improved identify energy criteria

Perspectives: BAMOS Juliette Laurent

Self-heating method: to perform fast characterization of the S-N curve for ropes

- ✓ Repeatability of the self-heating protocol validated
- ✓ Graphical fatigue prediction performed

→ Need of a model to understand the dissipation mechanisms: $\Delta^*_{material} + \Delta^*_{friction}$

→ **Fatigue prediction method for PA ropes using self-heating approach, to better understand the internal dissipation mechanisms for different load ratios**

Heat build-up protocol applied to higher scale sub-ropes

Heat build-up protocol to catch the influence of the load ratio on the fatigue properties

***L.Civier, Y.Chevillotte, C.Bain, G.Bles,.Y.Marco,P.Davies - Fatigue study of twisted polyamide sub-rope for floating wind turbines: Fast evaluation with heat build-up protocol and tomography study of mechanisms,* Ocean Engineering (2024)**

Perspectives: BAMOS

- **On the influencing parameters of PA ropes fatigue**
- **Challenge of a new fatigue criterion for synthetic ropes**

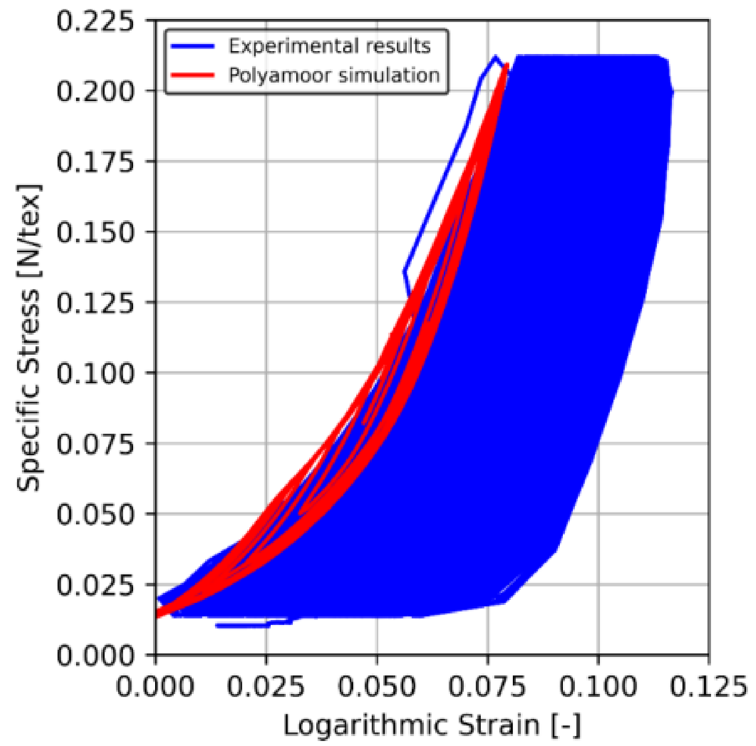

Questionable: only one test !

Table of contents

Development of a multi-scale model

FRANCE ENERGIES MARINES

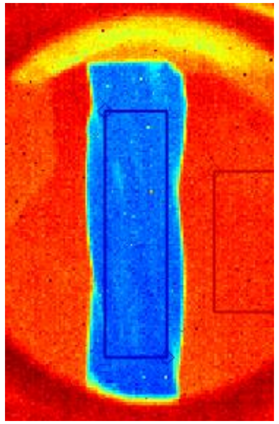

- Predict the impact of the construction parameter on the behavior/rigidity (strands diameter, lay-length, number of strands...)
- Understand the friction/abrasion

Multi-scale model

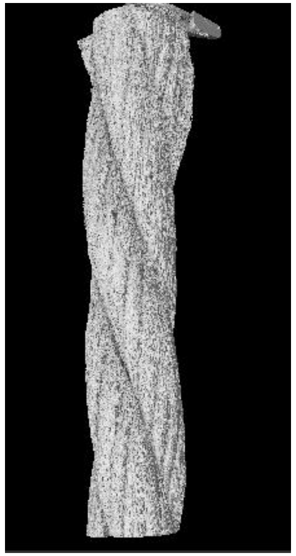

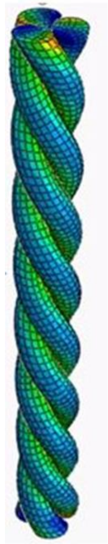

3D multi-scale model

Constitutive behaviour **+** **Friction**

$\Delta^*_{material}$ → **Measurements** ← $\Delta^*_{friction}$

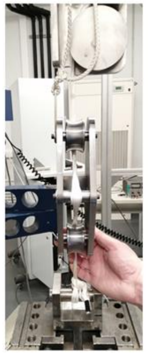

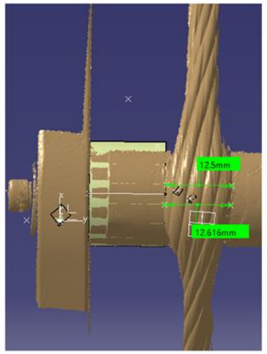

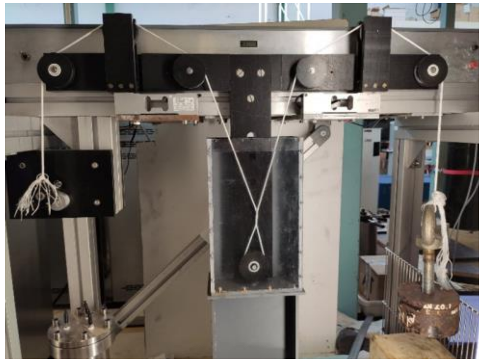

<u>Procedure followed:</u>

- Choice of a scale and approach
- Theoretical development
- Identification
- Validation

First definition of the law with hyper-elastic potential: no dissipation in the friction modes and no visco (elasto-plasticity).

Choice of the scale and objectives

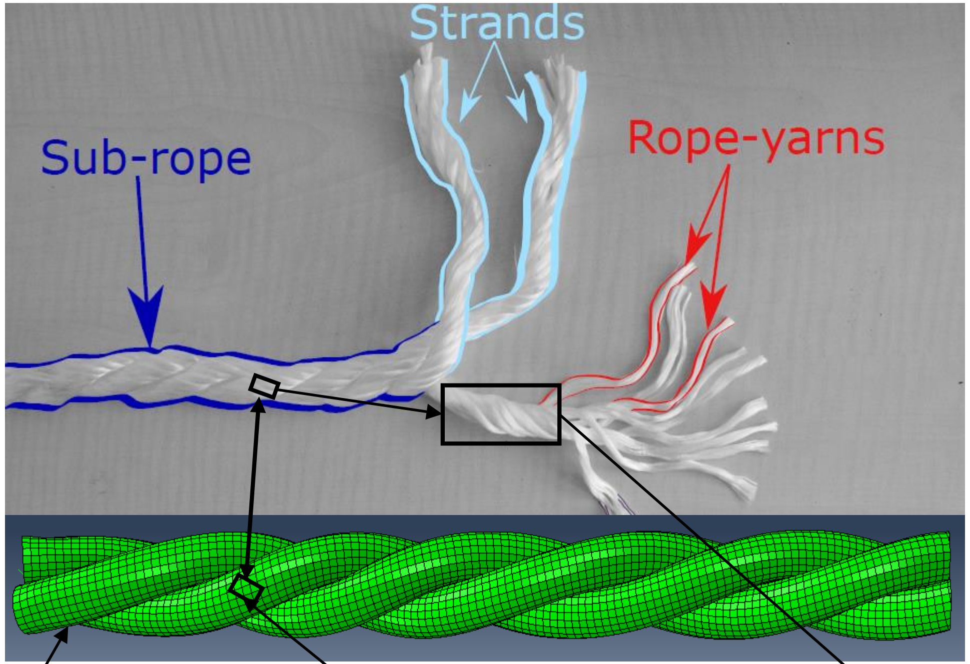

3 cylinders in contact

A behaviour law in all the integration points

Strands Scale:

➢ *3 cylinders in contact*

- Geometries
- Surfaces
- Inter-strand friction

Rope-yarns scale:

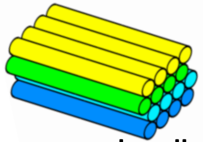

a bundle of rope-yarns

➢ *A behaviour law*

- Friction between rope-yarns (intra-strand frictions)
- Visco-elasto-plasticity
- Change of volume

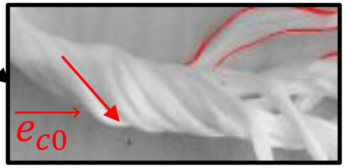

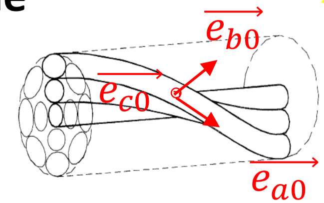

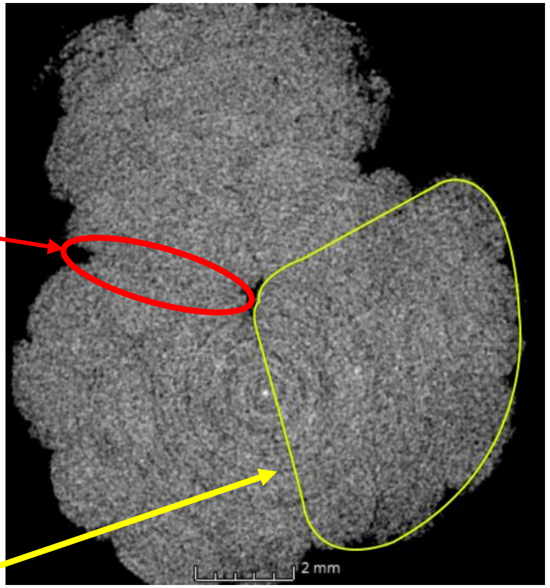

Which behaviour law ?

Chosen approach

Charmetant *et al. 2011.* A.Charmetant approach developed for the mechanical behaviour of textile composite reinforcements :

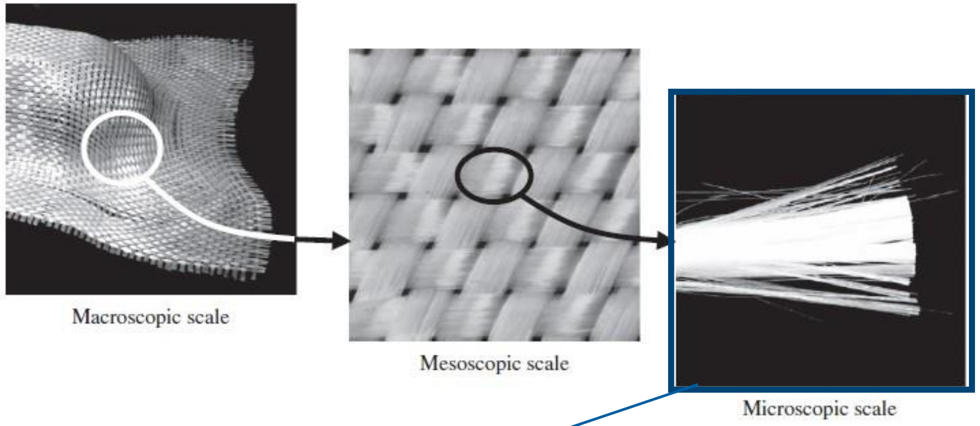

Anisotropic hyperelastic model:

- Homogeneous material corresponding to a bundle of fibres
- Material considered transversely isotropic
- Null intrinsic dissipation

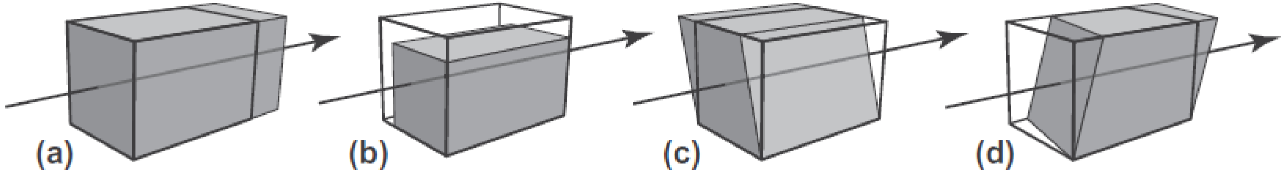

- Deformation decomposition valid in large deformation
- Choice of four scalar invariants strain-physically based to describe each deformation mode
- Choice of dedicated behaviour law for each deformation mode

Charmetant choice of invariants: Limited description of the shear strain modes

Adaptation of Charmetant's approach to completely describe the shear modes: **development of the FiBuLa law (fibre bundle law)**

Modelling the friction in a rope-yarn bundle

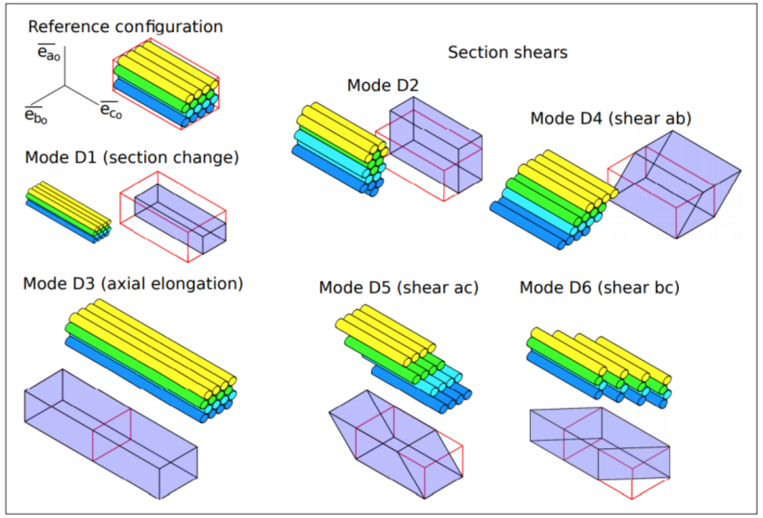

$$\widetilde{D_1} = \frac{1}{\sqrt{2}}\begin{bmatrix}1 & 0 & 0\\ 0 & 1 & 0\\ 0 & 0 & 0\end{bmatrix}_{(\bar{e}_{io})} \qquad \widetilde{D_2} = \frac{1}{\sqrt{2}}\begin{bmatrix}1 & 0 & 0\\ 0 & -1 & 0\\ 0 & 0 & 0\end{bmatrix}_{(\bar{e}_{io})}$$

$$\widetilde{D_3} = \begin{bmatrix}0 & 0 & 0\\ 0 & 0 & 0\\ 0 & 0 & 1\end{bmatrix}_{(\bar{e}_{io})} \qquad \widetilde{D_4} = \frac{1}{\sqrt{2}}\begin{bmatrix}0 & 1 & 0\\ 1 & 0 & 0\\ 0 & 0 & 1\end{bmatrix}_{(\bar{e}_{io})}$$

$$\widetilde{D_5} = \frac{1}{\sqrt{2}}\begin{bmatrix}0 & 0 & 1\\ 0 & 0 & 0\\ 1 & 0 & 0\end{bmatrix}_{(\bar{e}_{io})} \qquad \widetilde{D_6} = \frac{1}{\sqrt{2}}\begin{bmatrix}0 & 0 & 0\\ 0 & 0 & 1\\ 0 & 1 & 0\end{bmatrix}_{(\bar{e}_{io})}$$

In small deformation,
all deformation can be decomposed in 6 deformations modes:

$$\tilde{E} = \varepsilon_1\widetilde{D_1} + \varepsilon_2\widetilde{D_2} + \varepsilon_3\widetilde{D_3} + \varepsilon_4\widetilde{D_4} + \varepsilon_5\widetilde{D_5} + \varepsilon_6\widetilde{D_6}$$

With the set of tensor $\widetilde{D_i}$ an orthonormal basis of the vector space of the second-order symmetric tensors.

- **The longitudinal shears:** $(\boldsymbol{\varepsilon_5\widetilde{D_5} + \varepsilon_6\widetilde{D_6}})$
- **The transverse shears:** $(\boldsymbol{\varepsilon_2\widetilde{D_2} + \varepsilon_4\widetilde{D_4}})$

→ Deformation decomposition valid in large deformation

→ Choice of invariants that describe completely the 6 strain modes

Deformation decomposition

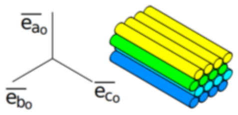

$\tilde{F}$ is the deformation gradient tensor to pass from the initial configuration Ω_0 to the current configuration Ω

$$\tilde{F} = \widetilde{R_\pi} \circ \widetilde{U_c} \circ \widetilde{U_{vol}} \circ \widetilde{U_{ab}} \circ \widetilde{K_\pi^{-1}}$$

Rope-yarns behaviour (deformation mode without shear)

$\widetilde{U_c}$

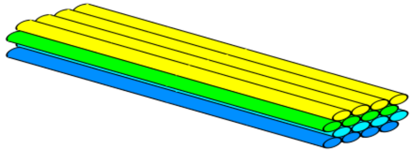

$\widetilde{U_{vol}}$

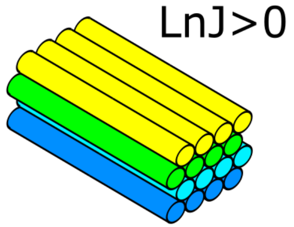

$$lnU_c = \ln\left(\frac{1}{\sqrt[3]{J}}\frac{c}{c_0}\right)$$

$$\ln J = \ln(\det \tilde{F})$$

Friction (shear deformation modes ($\widetilde{U_{ab}}$,$\widetilde{K_\pi^{-1}}$))

$\widetilde{U_{ab}}$

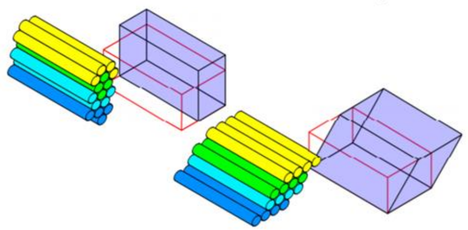

$\widetilde{K_\pi^{-1}}$

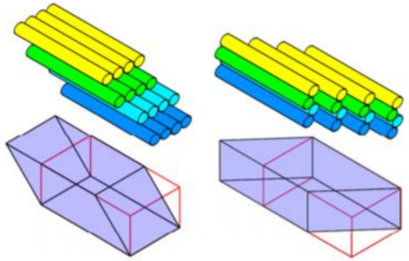

$$\ln \widetilde{U_{ab}} = \begin{bmatrix} lnU_{ab11} & lnU_{ab12} & 0 \\ lnU_{ab12} & -lnU_{ab11} & 0 \\ 0 & 0 & 0 \end{bmatrix}_{(\bar{e}_{io})}$$

$$\widetilde{\varepsilon_\delta} = \begin{bmatrix} 0 & 0 & \delta_a/2 \\ 0 & 0 & \delta_b/2 \\ \delta_a/2 & \delta_b/2 & 0 \end{bmatrix}_{(\bar{e}_{io})}$$

Obtention of the stress-strain FiBuLa law

FRANCE ENERGIES MARINES

Free specific energy:

$$\forall(\theta,\tilde{F})\ \psi(\theta,\ln J, Ln\ Uc, \widetilde{Ln\ U_{ab}}, \widetilde{\varepsilon_\delta}) = W_{Jc}(\theta, ln\ J, LnUc) + W_{ab}\left(\theta, \widetilde{Ln\ U_{ab}}\right) + W_\delta\left(\theta, \widetilde{\varepsilon_\delta}\right)$$

Thermodynamic

$$\forall(\theta,\tilde{F},\tilde{D})\ \tilde{\Sigma}:\tilde{D} = W'^{J}{}_{Jc} \cdot \dot{ln}\, J + W'^{c}{}_{Jc} \cdot Ln\dot{U}c + \widetilde{W'_{ab}} : \widetilde{Ln\dot{U}_{ab}} + \widetilde{W'_\delta} : \dot{\widetilde{\varepsilon_\delta}}$$

$$\text{with } \widetilde{W'_a} = \frac{\widetilde{\partial W_a}}{\partial\tilde{X}}(\theta,\tilde{X});\ W_a'^{x} = \frac{\partial W_a}{\partial x}(\theta,x,y)\ and\ W_a'^{y} = \frac{\partial W_a}{\partial y}(\theta,x,y)$$

Algebra

Stress-Strain law:

$$\forall(\theta,\tilde{F})\ \widetilde{R_\pi^T} \cdot \tilde{T} \cdot \widetilde{R_\pi} = \ldots$$

Identification of the axial elongation and change of volume mode

$$W_{Jc}(\theta, \ln J, LnUc)$$

4 parameters: a, b, c *and* d

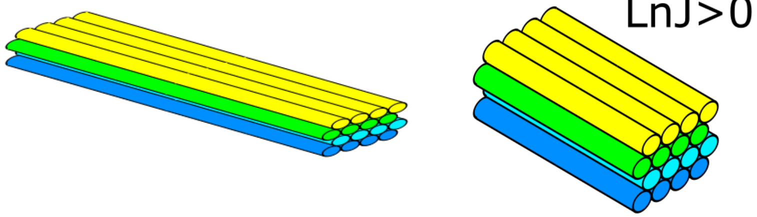

Capstan grips

Specifications:

- Test rope-yarns and strand
- Adapted terminations to distribute the load
- Test in water
- Monitoring of the axial and transversal strain

Experimental set-up:

- Capstan grips
- A rectangular tank full of water
- 2 cameras to measure the axial elongation
- 1 camera to measure the transversal strain
- 1 year of development

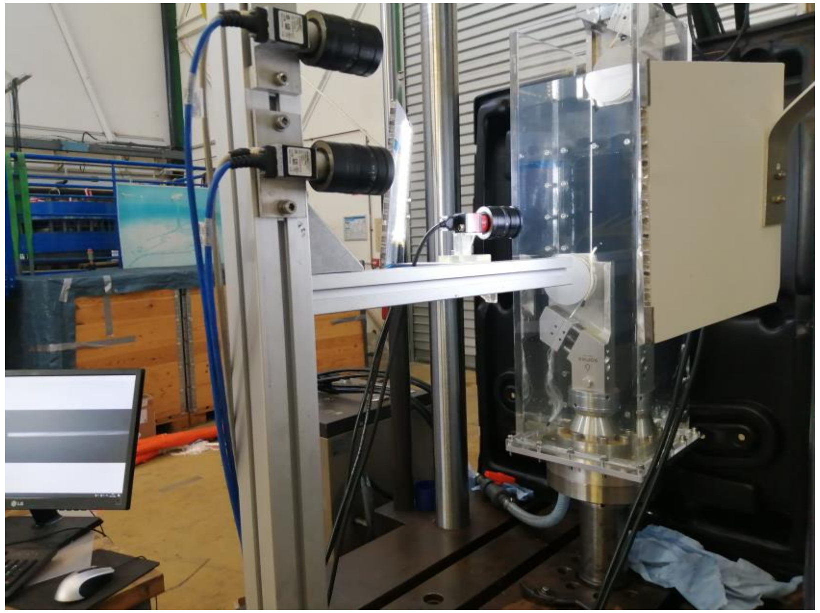

Experimental set-up

Experimental Identification of the shear strains modes

$W_{ab}\ (\theta, \widetilde{Ln\ U_{ab}})\ and\ W_{\delta}\ (\theta, \widetilde{\varepsilon_{\delta}})$

2 parameters: G_{ab} **and** G_{δ}

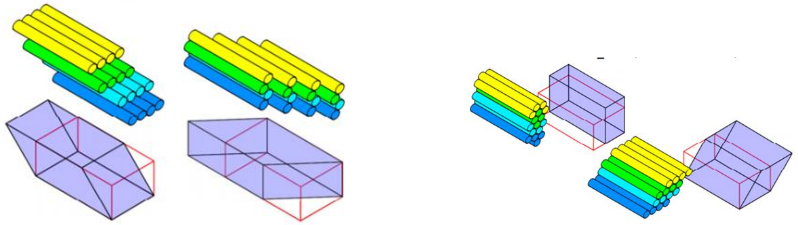

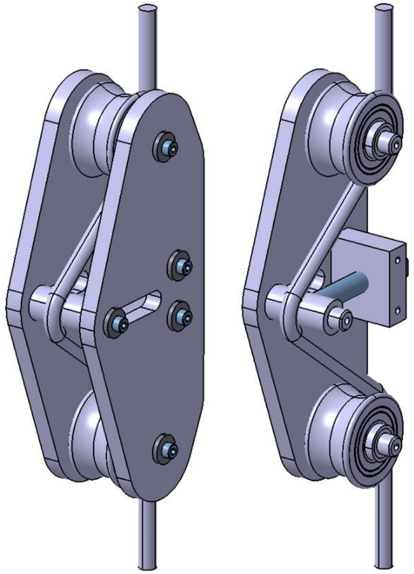

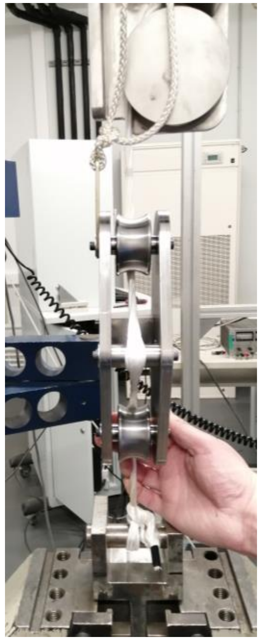

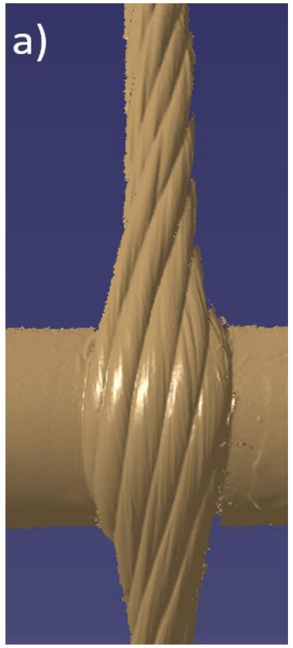

Specifications:

- Test a strand in the configuration « contact with a rod»
- Use the adequate monitoring to measure the contact between the rod and the strands

Experimental set-up:

- '3-rod' device conceived
- Tensile test with interruption each 2000 N
- 3D scan of the contact area

- 6 months of development

Inverse identification using the software Abaqus

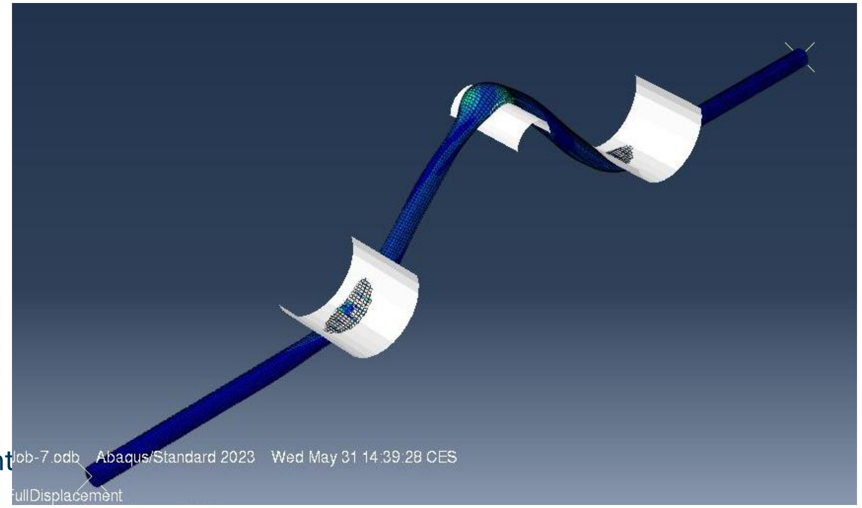

Identification of the shear strains modes

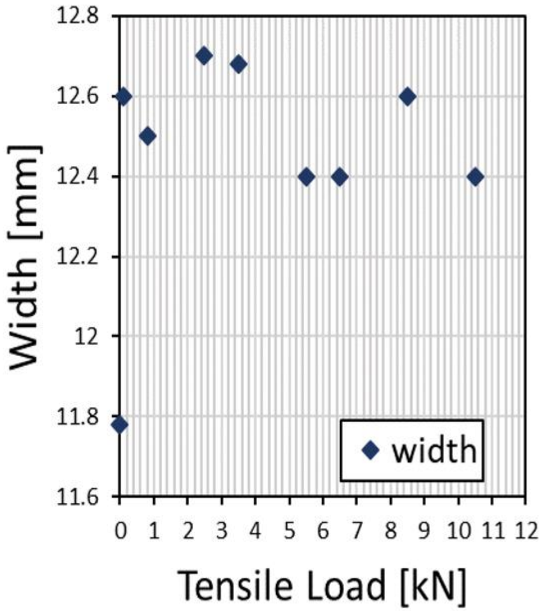

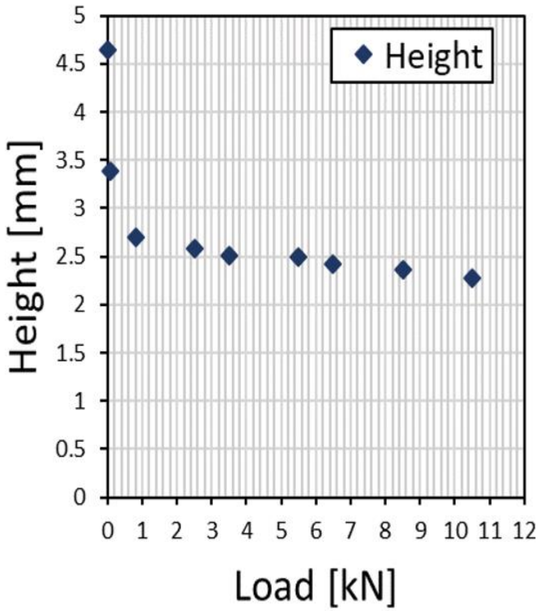

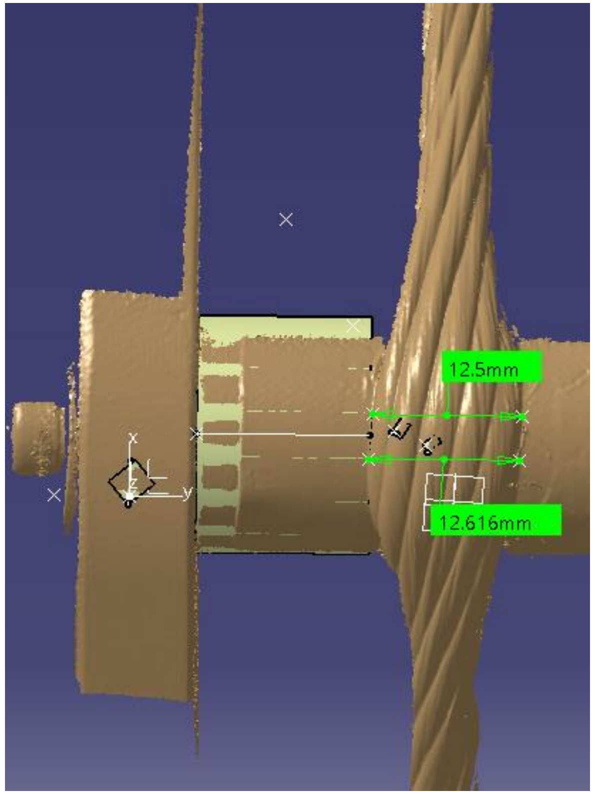

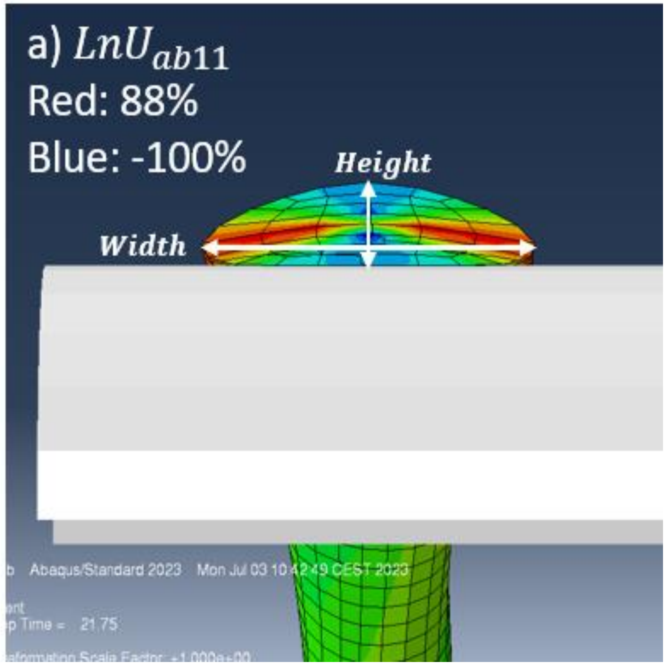

Strategy used:

Measurement of height and width every 2000 N during the tensile test

Simulation: Diametral Compression

- Implementation of the FiBuLa law on a UMAT for its use Abaqus™ software/Standard (Implicit algorithm)
  - Three steps in Abaqus/Standard (Implicit algorithm) and 22000 cubic elements (C3D8)

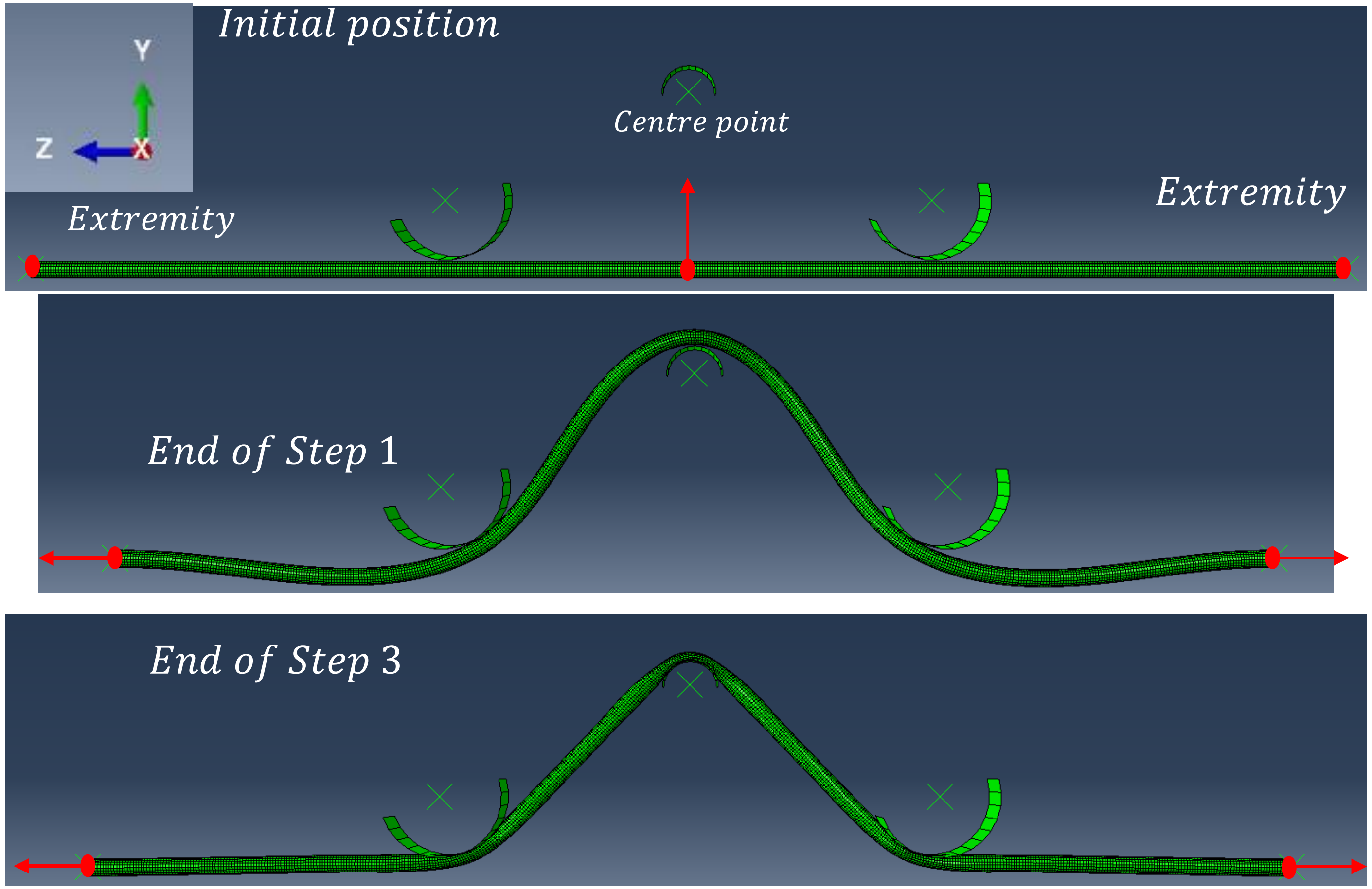

Simulation:A Diametral Compression

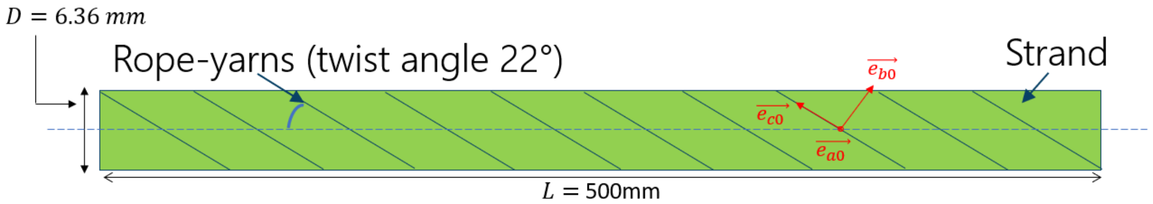

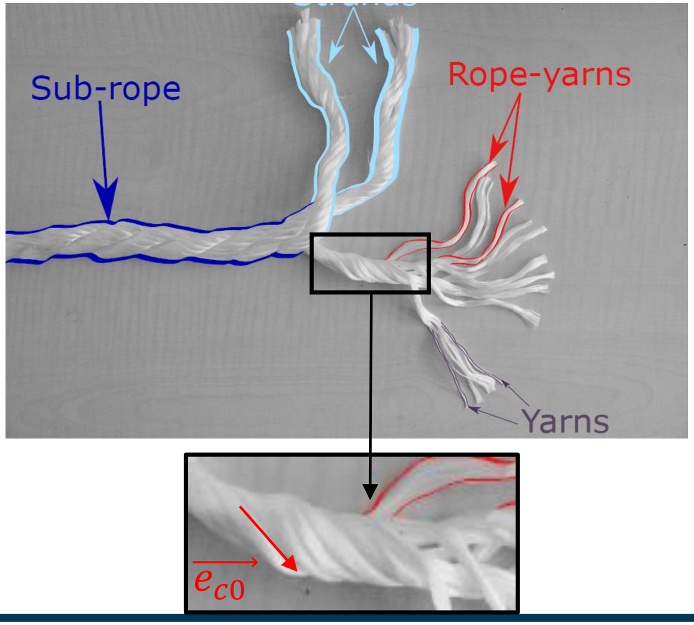

A parameter of the FiBuLa law:

- A point on the helix axis of the strand

Behaviour law implemented in each integration points:

- Determination of the position of the integration points regarding the point on the helix axis

- Calculation of the rope-yarn orientation using Leech (2002) description:

$$\cos\alpha_{RY} = \frac{1}{\sqrt{1 + (2 \cdot \pi \cdot p \cdot r_{RY})^2}}$$

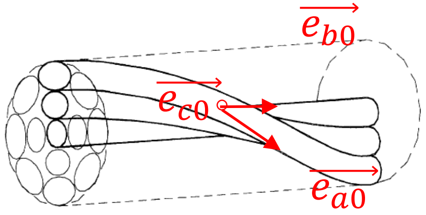

Characterization of one parameter: the friction coefficient

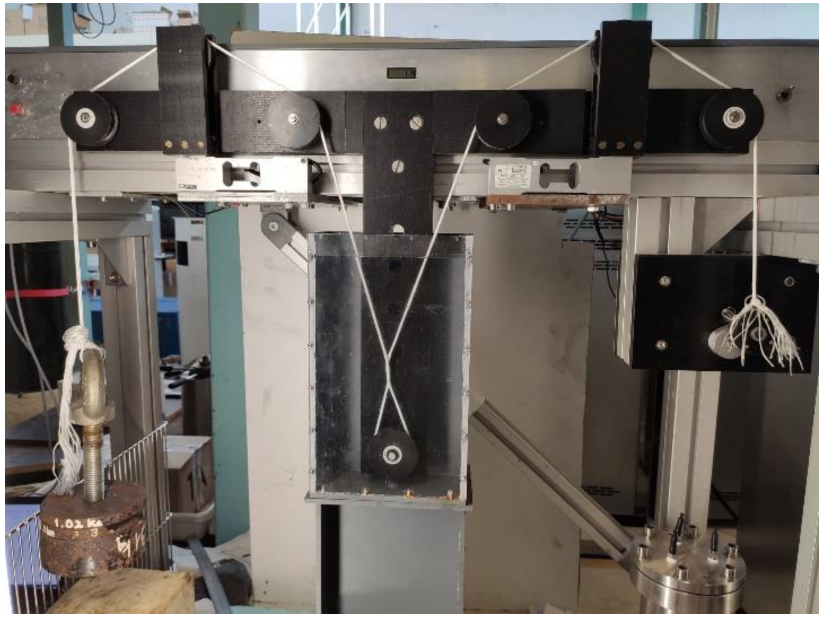

ASTM D3412-0 (γ small) type B. Cornelisssen et al. (2013)

Symetrical problem

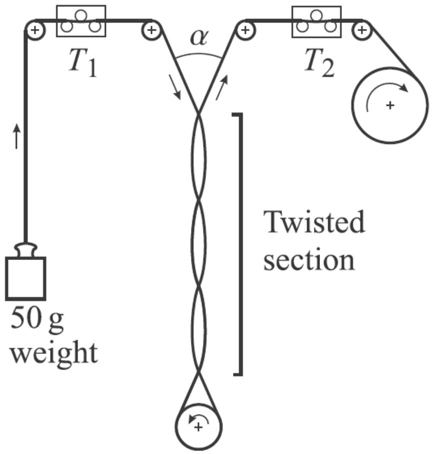

$$\mu = \ln\left(\frac{T_1}{T_2}\right)\frac{1}{2\pi n\gamma}$$

Hobbs analysis (2018):

No symmetry because T1 > T2

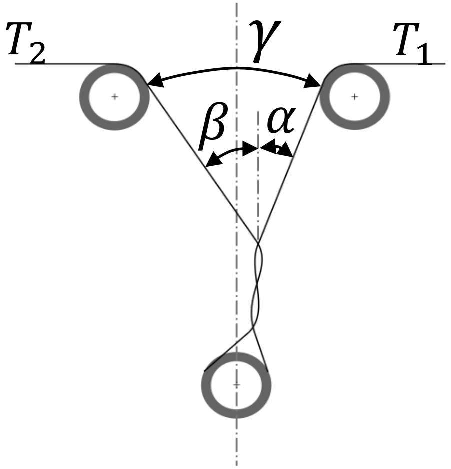

$$\mu = \frac{(T_1 - T_2)\tan\left(\gamma/_2\right)}{\pi(N_c - 1)(T_1\sin^2\alpha + T_2\sin^2\beta)}$$

- Experimental test bench for friction test: rope yarn on rope yarn at IFREMER, Brest

In literature, at filament scale (Gassara et al, 2018) : $\mu_l \approx 0{,}25$ 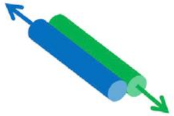 and $\mu_t \approx 0{,}17$ 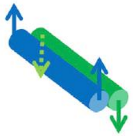

Characterization of one parameter: the friction coefficient

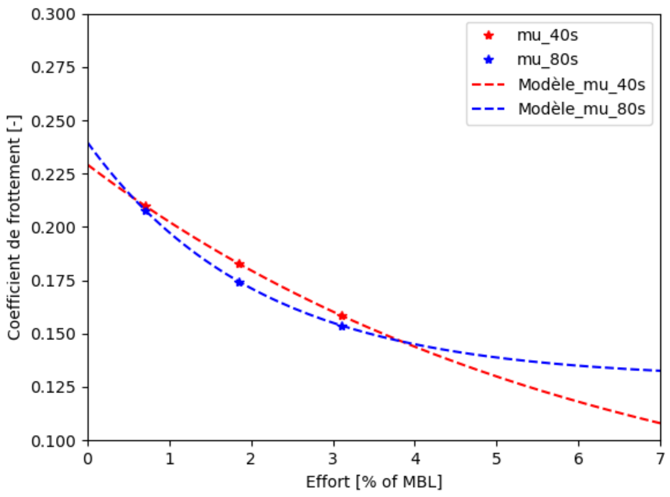

Article: C. Bain et *al. Experimental evaluation of the main parameters influencing friction between polyamide fibers and influence of friction on the abrasion resistance*

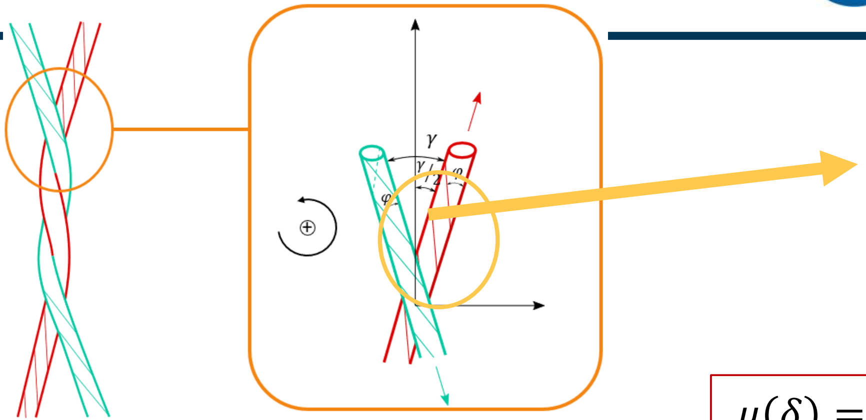

Scheme of the angle between fibres

$$\delta = \gamma - 2\varphi$$

$$\mu(\delta) = ae^{-b\delta} + c$$

The link could be explained by the angle betwen the yarns

$$\mu(F) = ae^{-bF} + c$$

$$\mu(\gamma) = a\tan^{-1}(b\gamma - c) + d$$

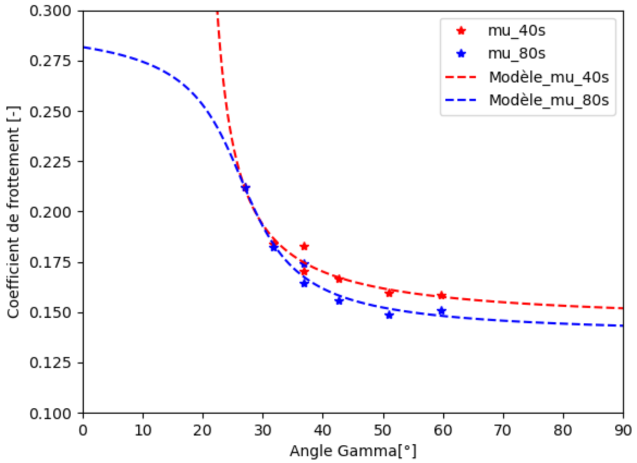

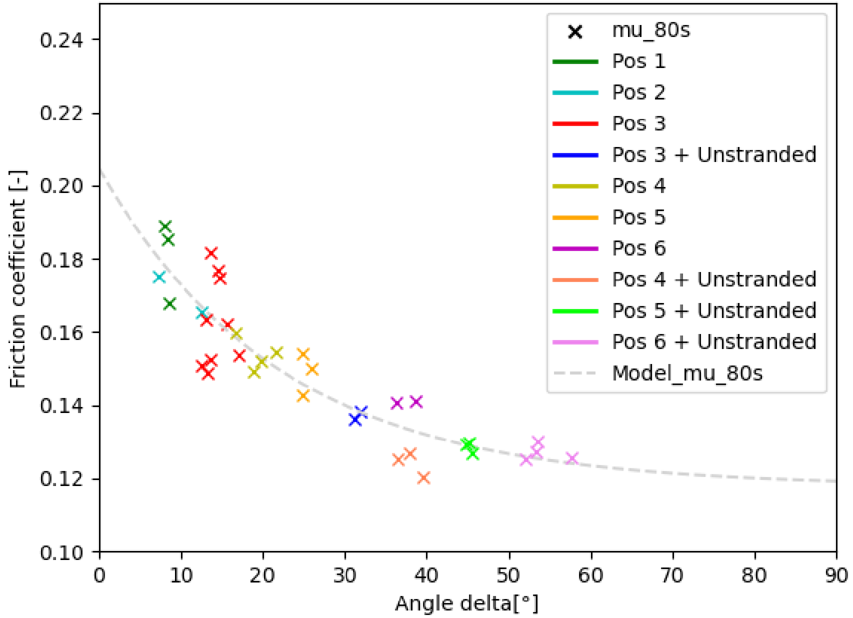

The inter-fibers angle δ and the friction angle β have been determined as the most important parameters controlling the friction coefficient for polyamide fibers.

First simulation of a sub-rope using the FiBuLa law

- Abaqus-Standard dynamic implicit analysis with option “quasi-static”
- Friction coefficient between strands: 0.15 (chosen using work Bain *et al. 2022.*)
- Cyclic loading (simulation duration: around 1 day)
- First comparison with experimental results

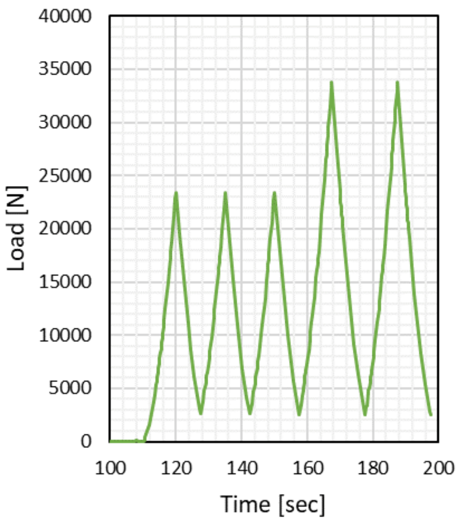

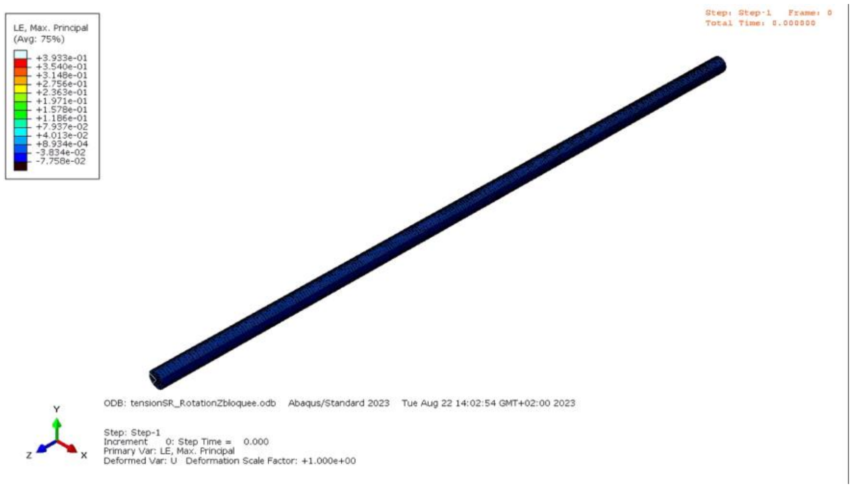

In service mean loading

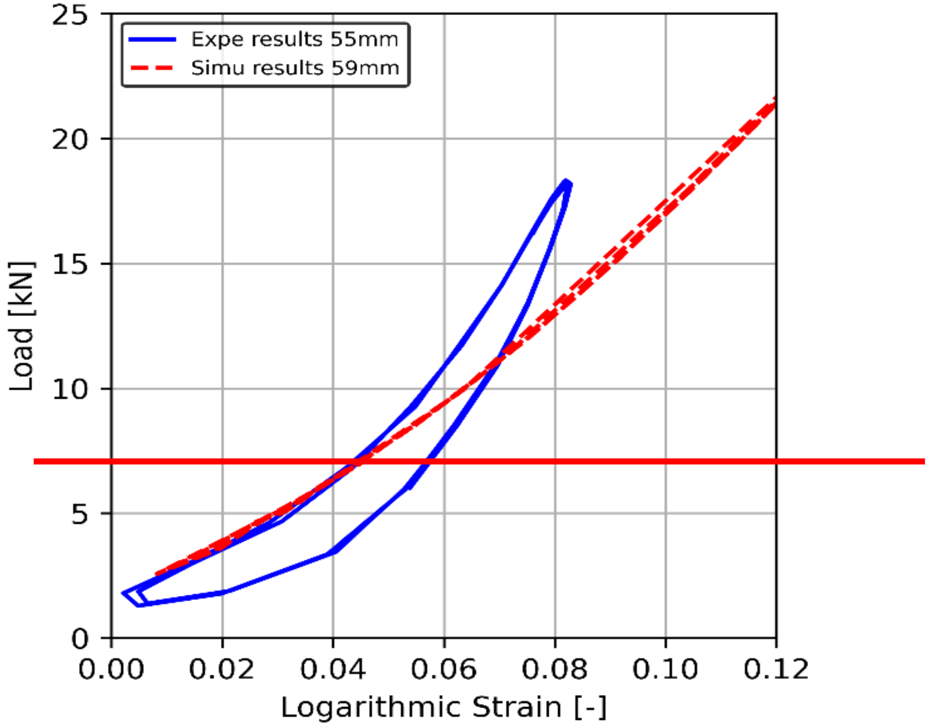

- The model is realistic though it underestimates the stiffness above 0.04 strain.
- No visible hysteresis on the model due to the friction between strands

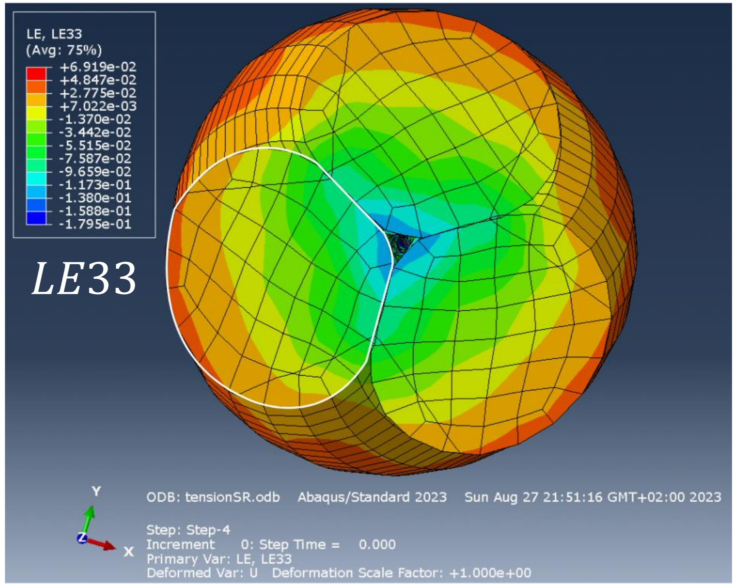

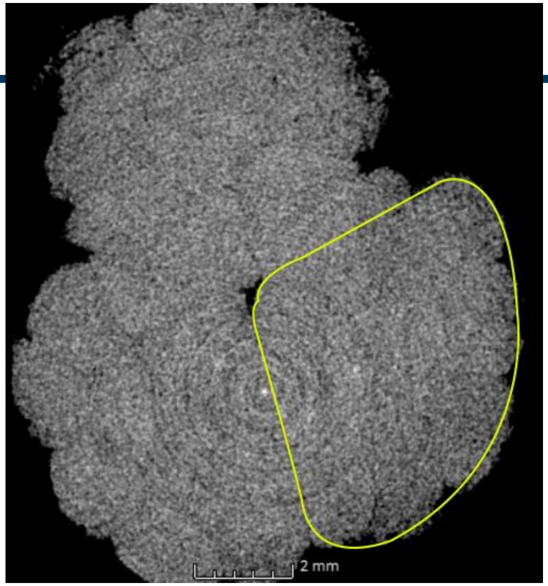

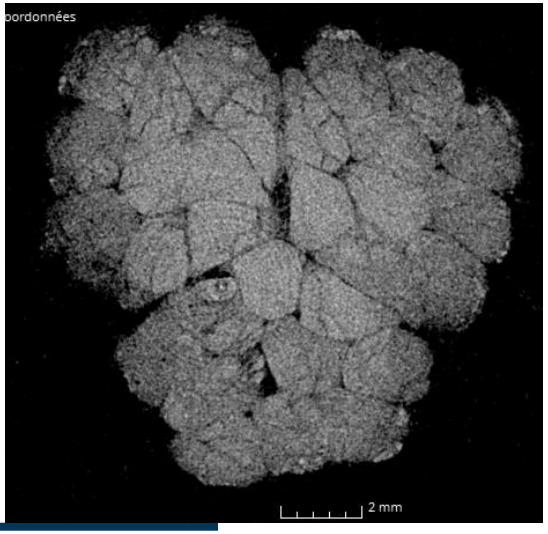

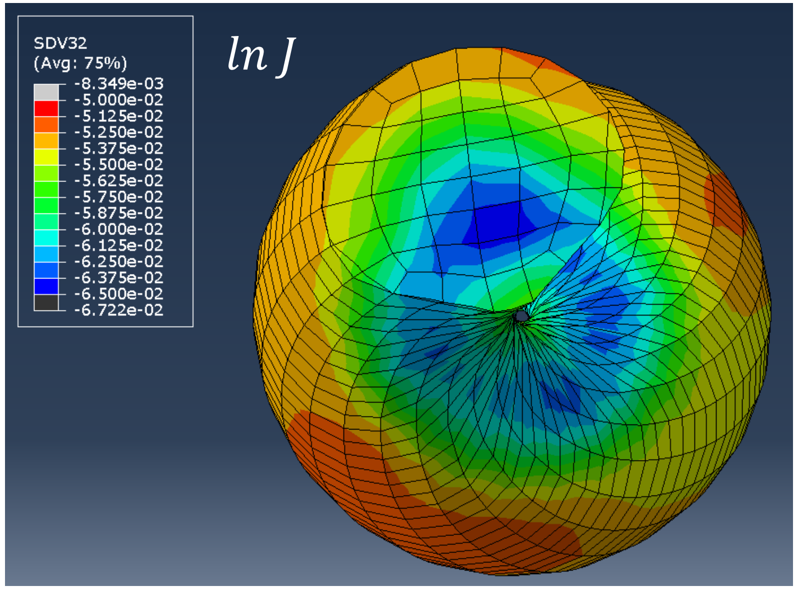

- ✓ Strong similarities between simulation and experimental shapes

- ✓ Rope-yarns subjected to more compression at the inner part of the sub-rope

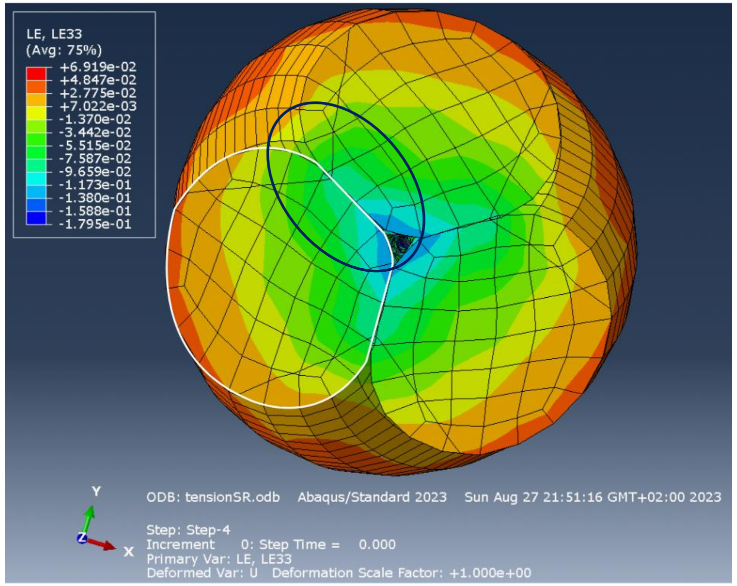

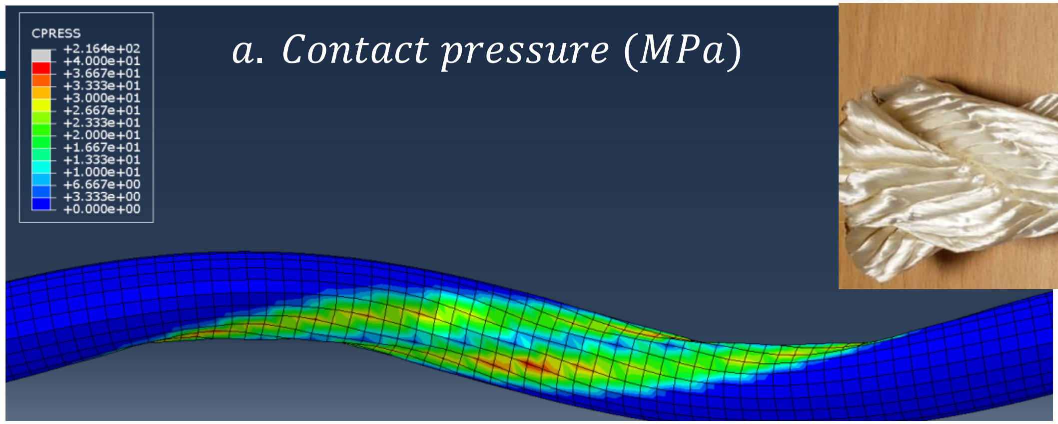

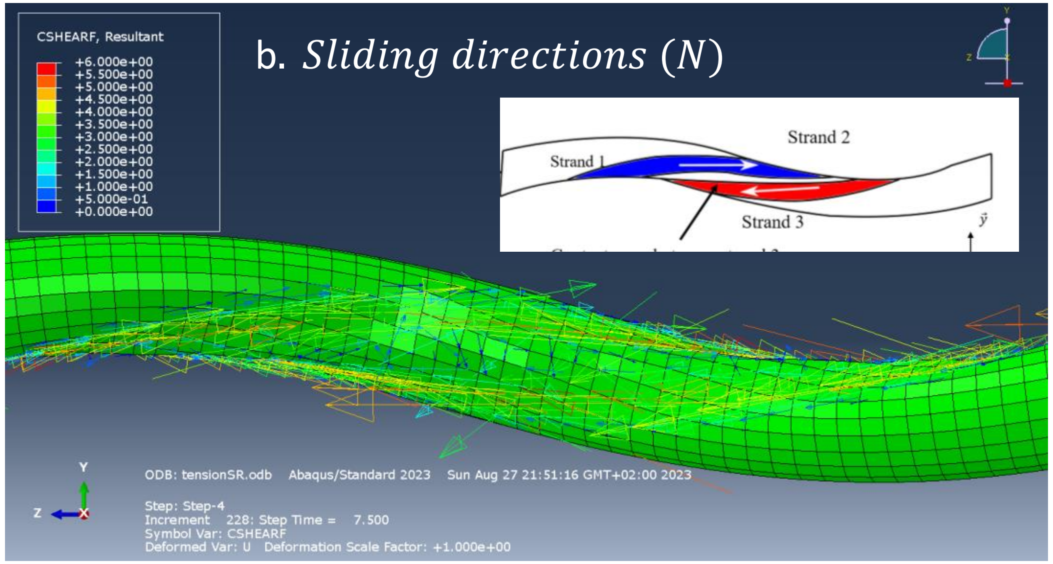

✓ The pressure and shear at the contact can be studied

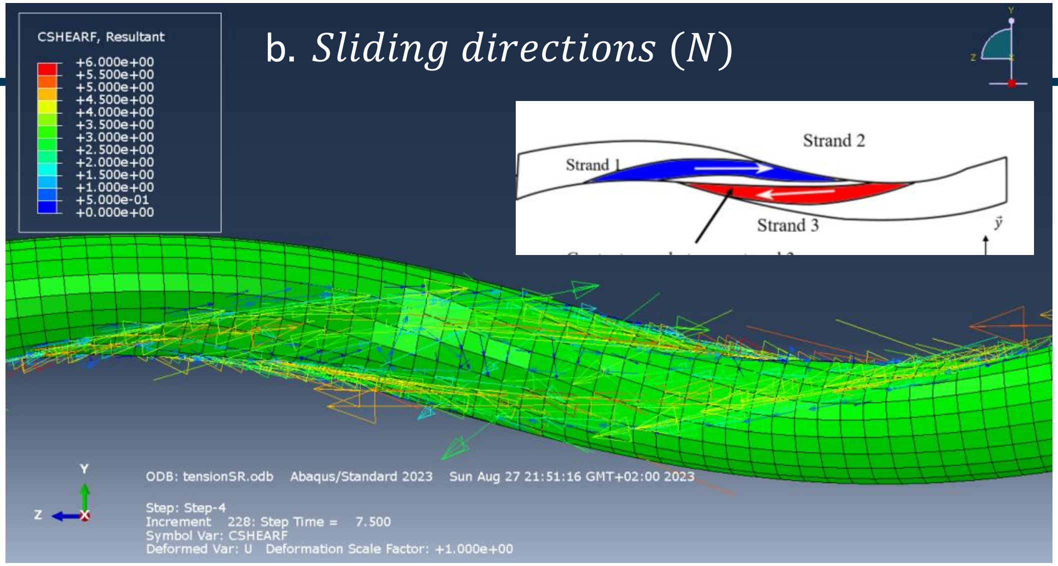

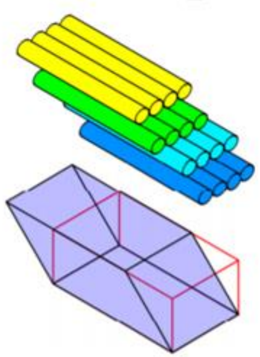

$$\widetilde{\varepsilon_\delta} = \begin{bmatrix} 0 & 0 & \delta_a/2 \\ 0 & 0 & \delta_b/2 \\ \boldsymbol{\delta_a/2} & \delta_b/2 & 0 \end{bmatrix}$$

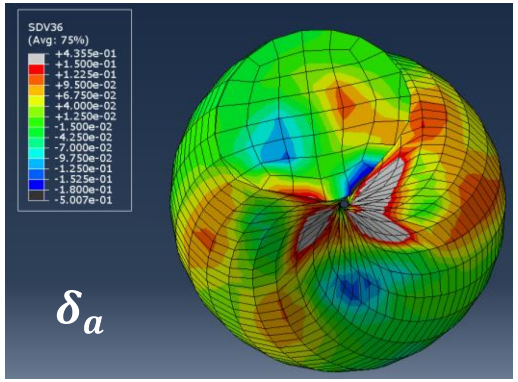

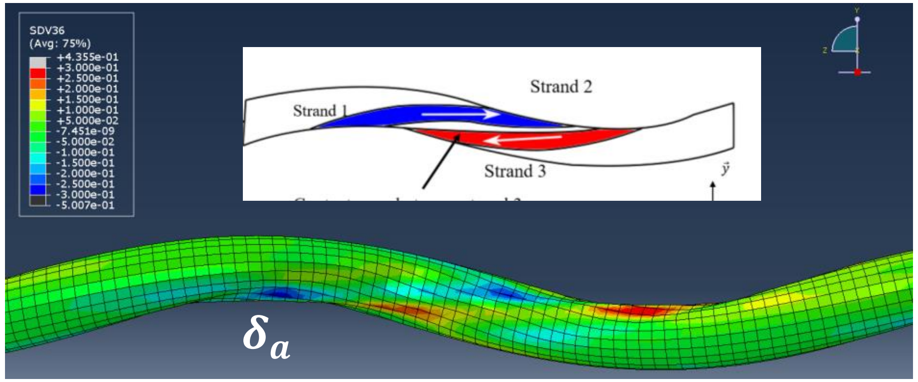

- ✓ δ_a induced by the contact with the other strands : same directions as the sliding directions of the strands obtained with Abaqus outputs

Conclusion on the MONAMOOR project

- Development of the FiBuLa law: adaptation of A.Charmetant model to a 3-stranded polyamide sub-rope
- Development of original experimental set-ups for the experimental identifications of the parameters
- Implementation in a FORTRAN UMAT for the first calculation on Abaqus software
- First simulation of a sub-rope:
  - At the strands scale: obtention of the geometries, contact forces and sliding directions
  - At the rope-yarns scale: coherent prediction of the strain fields and new insights

→ The model is a precious tool to understand the mechanics of rope

→ The model could allow to separate the dissipation due to friction from the dissipation due to the material

Perspectives BAMOS: PhD Juliette Laurent

Development of a meso-scale model

- Addition of the POLYAMOOR 1D law to the meso-scale model, identified on rope-yarns (instead of the current 1D elastic law)
- Inclusion of friction between rope-yarns (changing the current 2D elastic law for a 2D elasto-plastic law)
- Identification and validation of the meso-scale model performed on the MONAMOOR experimental campaign and on new tests (other scales, other construction)